Lithocholic acid-based design of noncalcemic vitamin D receptor agonists

Sunil Gaikwad, Carmen González, Daniel Vilariño, Gonzalo Lasanta, Carmen Villaverde, Antonio Mouriño, Lieve Verlinden, Annemieke Verstuyf, Carole Peluso-Iltis, Natacha Rochel, et al.

Lithocholic Acid-Based Design of Noncalcemic Vitamin D Receptor Agonists

Sunil Gaikwad[‡,ψ] Carmen M. González,[‡,¶] Daniel Vilariño,[‡] Gonzalo Lasanta.[‡] Carmen Villaverde,[‡,†] Antonio Mouriño,[*,‡] Lieve Verlinden,[§] Annemieke Verstuyf,[§] Carole Peluso-Iltis,[ƒ] Natacha Rochel,[*,ƒ] Klaudia Berkowska, [ξ] Ewa Marcinkowska[*,ξ]

[‡]Departamento de Química Orgánica, Laboratorio de Investigación Ignacio Ribas, Universidad de Santiago de Compostela, Avda das Ciencias s/n, 15782 Santiago de Compostela, Spain.

[ξ] Laboratory of Protein Biochemistry, Faculty of Biotechnology, University of Wrocław, Joliot-Curie 14a, 50-383 Wrocław, Poland.

[§]Clinical and Experimental Endocrinology, Department od Clinical and Experimental Medicine, KU Leuven, Herestraat 49, bus 9802, 3000 Leuven, Belgium.

[ƒ]Institut de Génétique et de Biologie Moléculaire et Cellulaire (IGBMC), 67400 Illkirch, France; Institut National de La Santé et de La Recherche Médicale (INSERM), U1258, 67400 Illkirch, France; Centre National de Recherche Scientifique (CNRS), UMR7104, 67400 Illkirch, France; Université de Strasbourg, 67400 Illkirch, France.

*Corresponding authors:
Antonio Mourino: antonio.mourino@usc.es
Natacha Rochel: rochel@igbmc.fr
Ewa Marcinkowska: ema@cs.uni.wroc.pl

[ψ] Present address: Department of Chemistry, Centre for Advanced Research, Savitribai Phule Pune University, Pune-411007, India.

[¶] On sabbatical leave from the Benemerita Universidad Autónoma de Puebla (BUAP), Mexico.

[†]Deceased

ABSTRACT: The hypercalcemic effects of the hormone 1α,25-dihydroxyvitamin D_3 (calcitriol) and most of known vitamin D metabolites and analogs call for the development of non secosteroidal vitamin D receptor (VDR) ligands as new selective and noncalcemic agonists for treatment of hyperproliferative diseases. We report on the *in silico* design and stereoselective synthesis of six lithocholic acid derivatives as well as on the calcemic activity of a potent LCA derivative and its crystallographic structure in complex with zVDR LBD. The low calcemic activity of this compound in comparison with the native hormone makes it of potential therapeutic value. Structure-function relationships provide the basis for the development of even more potent and selective lithocholic acid-based VDR ligands.

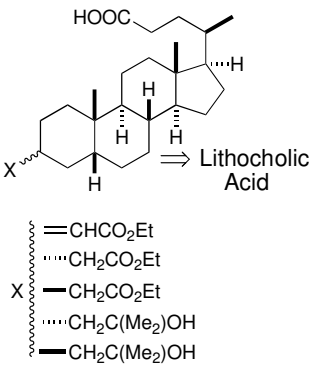

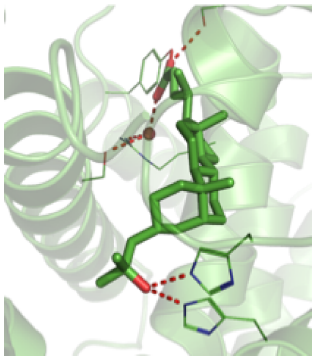

1. Introduction

The vitamin D receptor (VDR) is a transcription factor that belongs to the nuclear receptor superfamily and exerts its biological functions through its natural ligand 1α,25-dihydroxyvitamin D_3 [calcitriol, 1,25-$(OH)_2D_3$, 1,25D, Fig. 1], which is the hormonally active form of vitamin D_3 [1,2]. VDR acts as a heterodimer with the retinoid X receptor (RXR). Upon ligand binding, the VDR undergoes a conformational change at helix 12 (H12) allowing the heterodimer RXR-VDR to bind to specific DNA sequences (Vitamin D response elements [VDREs]) and to interact with various coactivator proteins that regulate access to transcriptional target genes [3]. As a result multiple biological functions are achieved including regulation of bone mineralization, calcium/ phosphate homeostasis, cell growth, cell differentiation/ proliferation, apoptosis and immune responses [4-5]. The fact that the VDR has been found in more than 30 target tissues and cell tumors has suggested that it might mediate an even wider array of biological functions including cancer prevention [6,7]. The biological actions mediated by the VDR have pointed to this receptor as a possible therapeutic target for therapy of hyperproliferative disorders [4,5]. Unfortunately, the clinical use of the native hormone 1,25D for cancer treatment has been limited by the induction of high levels of calcium (hypercalcemia) [4]. A number of highly active noncalcemic secosteroidal VDR ligands have been developed [8,9] and some of them have already found clinical applications [9-11], but with limited success in cancer treatment because the required pharmacological doses induce toxicity. Most of these VDR ligands are secosteroidal vitamin D analogs structurally modified at the side-chain, A-ring, and CD-rings [review in 8-9]. A few examples of this class of compounds include Calcipotriol (MC903) [12], ILX23-7553 [13], XE4MeCF3 [14], PG-136 [15], Paricalcitol (Zemplar) [16], Inecalcitol (TX522) [17], and Mart-10 [18] (Fig. 1). Another group of promising VDR agonists with potential therapeutic applications include easily synthesized nonsteroidal compounds that mimic the biological potency of the native hormone 1,25D without displaying calcemic action (review in [9,19-20]. Selected ligands of this group of VDR ligands include LG190178 [21], CD4849 [22], and *p*-carborane CB-31 [23] (Fig. 1). In addition non-calcemic vitamin D hydroxyderivatives have been shown to act as biased VDR agonists [24]. Other ligands that bind to VDR include 3-arylbenzopyranes [25], 1α,25$(OH)_2$-lumisterol$_3$ [26], podocarpic acid derivatives [27], and natural bile acid compounds such as lithocholic acid (**1a**, LCA, Fig. 2) [28].

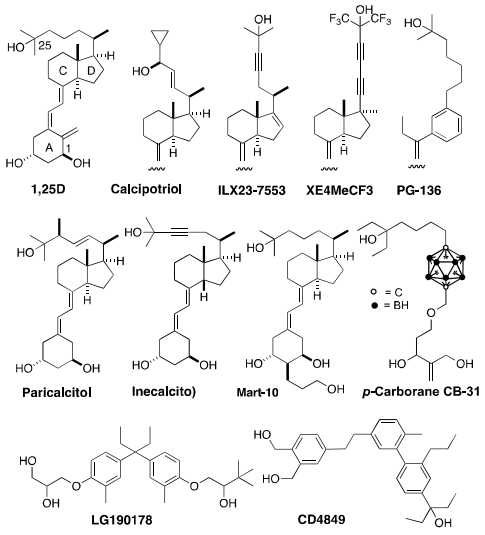

Fig. 1. Structure of the natural hormone 1α,25-dihydroxyvitain D_3 (1,25D), selected noncalcemic 1,25D analogs and nonsteroidal mimics.

On the basis of the crystal structures of 1,25D and other ligands bound to the ligand binding domain of hVDR [29], we designed by molecular docking and synthesized secosteroidal superagonist ligands of therapeutic potential [30]. However, the mechanism by which structurally different vitamin D analogs are noncalcemic continues to be largely unexplained [5,11]. Assuming that VDR ligands with a high degree of locked conformations would induce a limited number of biological actions, we started two decades ago a research program focused on the synthesis and biological evaluation of vitamin D analogs with partially locked side-chains to gain insights into the genes involved in structure-function selectivity [31]. As a continuation of this program we focused here on lithocholic acid (**1a**, LCA, Fig. 2), which is a natural VDR ligand with a high degree of conformational rigidity due to the steroidal A, B, C and D rings, the carboxylic side-chain being the only flexible part of the molecule. LCA, which is involved in the development of colon cancer, binds to VDR with low-affinity to induce expression of CYP3A, a cytochrome P450 enzyme involved in the detoxification of LCA [32]. This bile acid can also carry out vitamin D functions such elevation of calcium levels and mobilization of calcium from bone [33]. It has also been reported that LCA displays anti-carcinogenic properties in several cancer cell models [34,35] and controls adaptive immunity via inhibition of Th1 activation [36]. The LCA synthetic derivatives, LCA acetate (1b) and LCA propionate (1c), (Fig. 2), induce bile acid metabolism and cell growth control more efficiently than LCA (1a) without inducing hypercalcemia [37]. The recent report by H. Sasaki et al. on LCA derivatives modified at the A-ring as vitamin D receptor agonists [38], prompted as to disclose our results on the design, synthesis, biological evaluation and characterization of LCA derivatives modified at the steroidal A-ring.

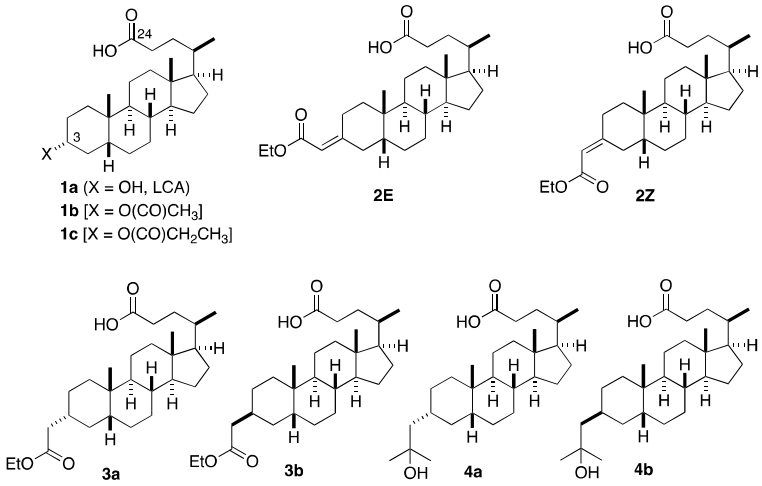

Fig. 2. Structures of lithocholic acid (**1a**, LCA), known LCA-derivatives **1b**, **1c**, and target LCA-derivatives **2E**, **2Z**, **3a**, **3b**, **4a**, **4b**.

2. Results and discussion

2.1. Design

The crystal structures of LCA (**1a)** and its LCA derivatives **1b** and **1c** in complex with rat VDR LBD show that these ligands are accommodated in the VDR-binding pocket as the native ligand 1,25D, but in the opposite orientation [39]. The side-chain-COOH group occupies the VDR LBD region corresponding to the A-ring of 1,25D, while the OH and ester groups face the helix 12 (H12). Interestingly, the crystal structure of LCA in complex with zebrafish VDR LBD reveals two different binding sites, one inside the zVDR LBD, and another on the surface of the zVDR LBD. In both crystal structures (LCA-rVDR LBD and LCA-zVDR LBD), the steroidal A-ring-OH groups bind weakly via water-mediated hydrogen bonding to rHis301 (H6) and rHis393 (H11), and to zHis333 and zHis423, respectively [40]. In this work we replace the water molecules that mediate hydrogen bonding between LCA (OH group) and zVDR LBD (zHis333 and zHis423) by hydroxy-alkyl, alkyl-ester, and alkenyl-ester fragments to increase ligand-receptor binding and biological potency of the ligand. With a view on a possible treatment of hyperproliferative disorders, we expected that the steroidal rigidity of the new LCA derivatives **2Z**, **2E**, **3a**, **3b**, including the recent reported **4a**, and **4b** [38], could induce a low or negligible calcemic action in comparison with the natural hormone 1,25D.

The new LCA derivatives **2Z-4b** were docked into the LBD derived from the X-ray crystal structure of the complex 1,25D-hVDR LBD [29] using the Gold program. The results of our docking calculations for each LCA derivative and the corresponding superimposition with the natural hormone 1,25D are shown in Figure 3. The carboxylic side chain occupies the A-ring region corresponding to the natural hormone 1,25D, while the C3-alkyl, C3-alkenyl-ester, and the C3-hydroxy-alkyl functionalities attached to the LCA-A-ring interact by hydrogen-bonding with His305 and His397. In all cases the docked conformations were superimposed with that of the natural hormone 1,25D. Relative binding scoring of each LCA derivative including the parent LCA (**1a**, SI) in comparison with 1,25D (100%, SI) are LCA (74%), **2Z** (64%), **2E** (72%), **3a** (78%), **3b** (76%), **4a** (80%), **4b** (77%). Compound **4a** binds best to the hVDR LBD and also adopts the conformation that best overlaps with the natural hormone, in particular its side chain and D-ring. The A-ring hydroxyl group of **4a** is similarly positioned as the 25-OH group of 1,25D, forming effective hydrogen bonds with His-305 and His-397, Ser-278, Arg-274, Tyr-143, and expected to efficiently stabilize the VDR agonist conformation.

A)

2E (72%)

AA	A
TYR-147	3.7
PHE-150	3.8
LEU-227	3.9
LEU-230	3.5
ALA-231	3.7
LEU-233	2.9
VAL-234	3.8
ILE-268	3.9
ILE-271	3.3
SER-275	3.0
TRP-286	3.4
CYS-288	3.5
TYR-295	2.7
VAL-300	3.6
LEU-313	4.1
VAL-418	3.7

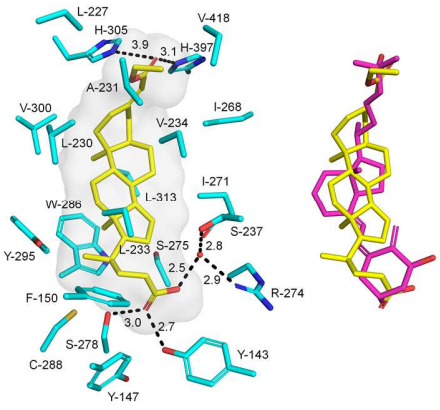

2Z (64%)

AA	A
TYR-147	3.6
LEU-227	3.7
LEU-230	3.2
LEU-233	3.6
VAL-234	2.2
ILE-271	2.9
SER-275	3.3
TRP-286	3.5
CYS-288	4.2
TYR-295	2.7
VAL-300	4.3
ALA-303	4.2
LEU-313	4.2
TYR-401	3.3
LEU-404	4.0
LEU-414	3.7
VAL-418	3.3
PHE-422	3.6

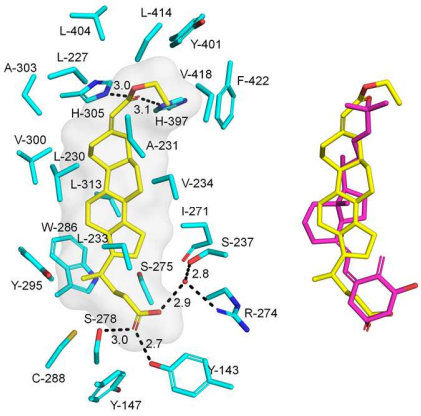

B)

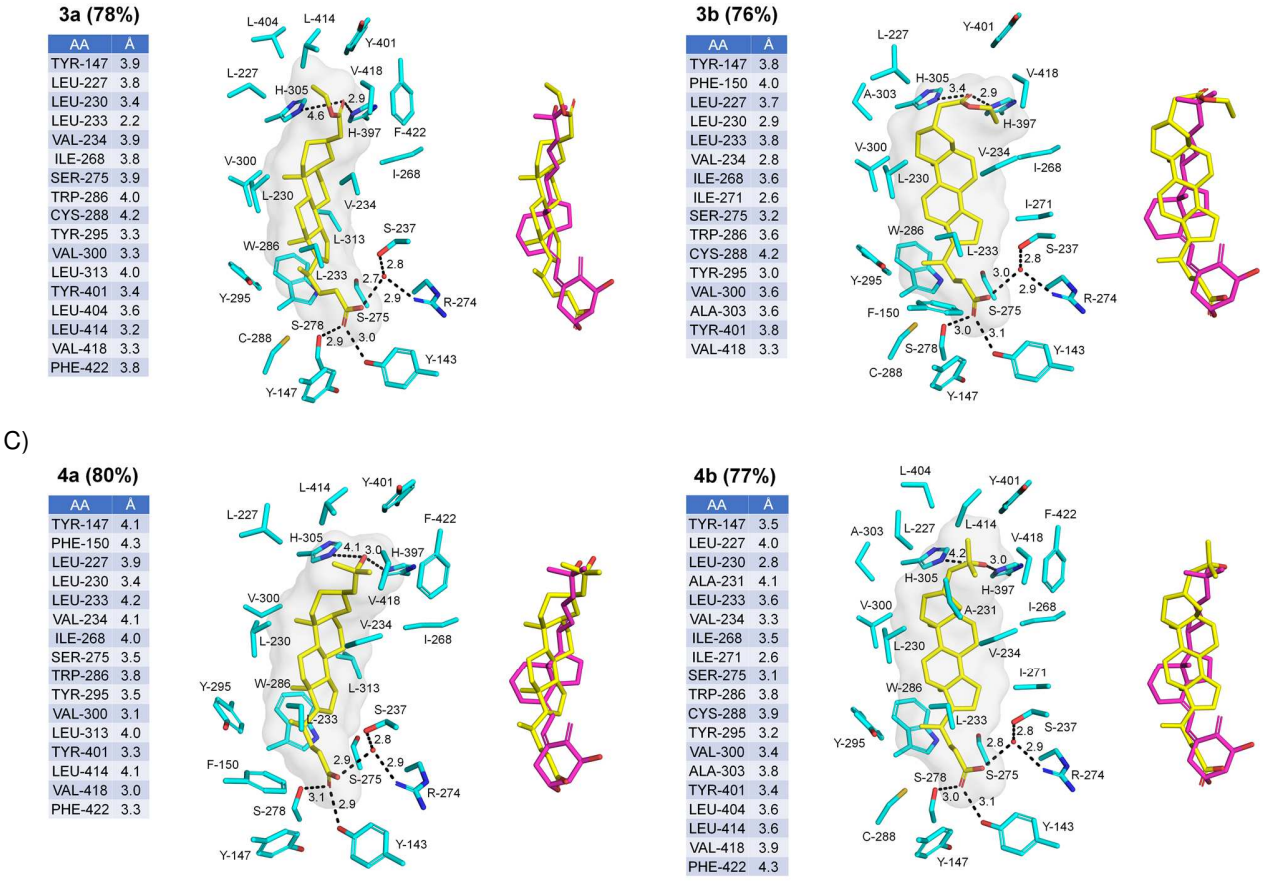

Fig. 3. Docked structures of ligands **2E**, **2Z**, **3a**, **3b** **4a**, and **4b** (yellow) into hVDR LBD and their superimposition with the natural hormone 1,25D (magenta). A (**2E** and **2Z)**. B (**3a** and **3b)**. C (**4a** and **4b)**. Relative binding scoring in comparison with 1,25D (100%) are shown in parenthesis.

2.2. Chemistry

The retrosynthetic analysis of the target compounds **2E**, **2Z**, **3a**, **3b, 4a**, **4b** is depicted in Scheme 1. The synthesis of the target compounds was envisioned to arise from known diol **6** [41], which could be transformed into unsaturated esters **5E** and **5Z** by regioselective protection and Wadsworth-Horner-Emmonds chemistry. Desilylation of these esters followed by oxidation would provide the target compounds **2E** and **2Z**. Esters **5E** and **5Z** could be converted to intermediates **7a**(3*R*) by catalytic hydrogenation from the less sterically hindered face followed by deprotection. Compounds **7a** and **7b** could also be individually prepared by catalytic diastereoselective reduction of either **5E** or **5Z**. Desilylation-oxidation of **7a** or **7b** would provide the target compounds **3a** and **3b**, respectively. Target compounds **4a** and **4b** would arise from **7a** or **7b** through the respective diols **8a** or **8b** employing the same oxidation sequence.

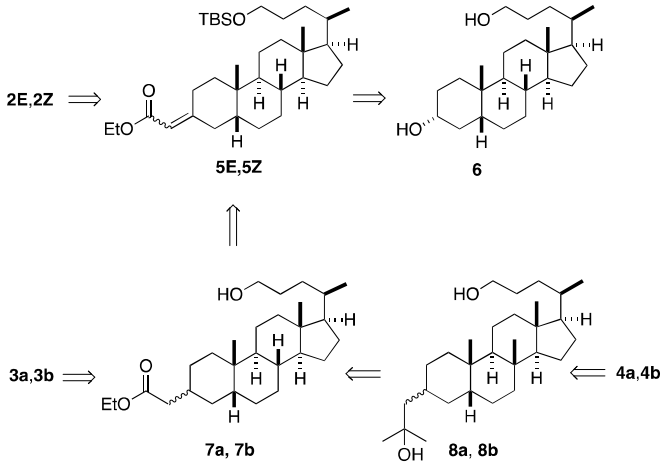

Scheme 1. Retrosynthetic analysis of the target compounds **2E**, **2Z**, **3a**, **3b, 4a**, and **4**

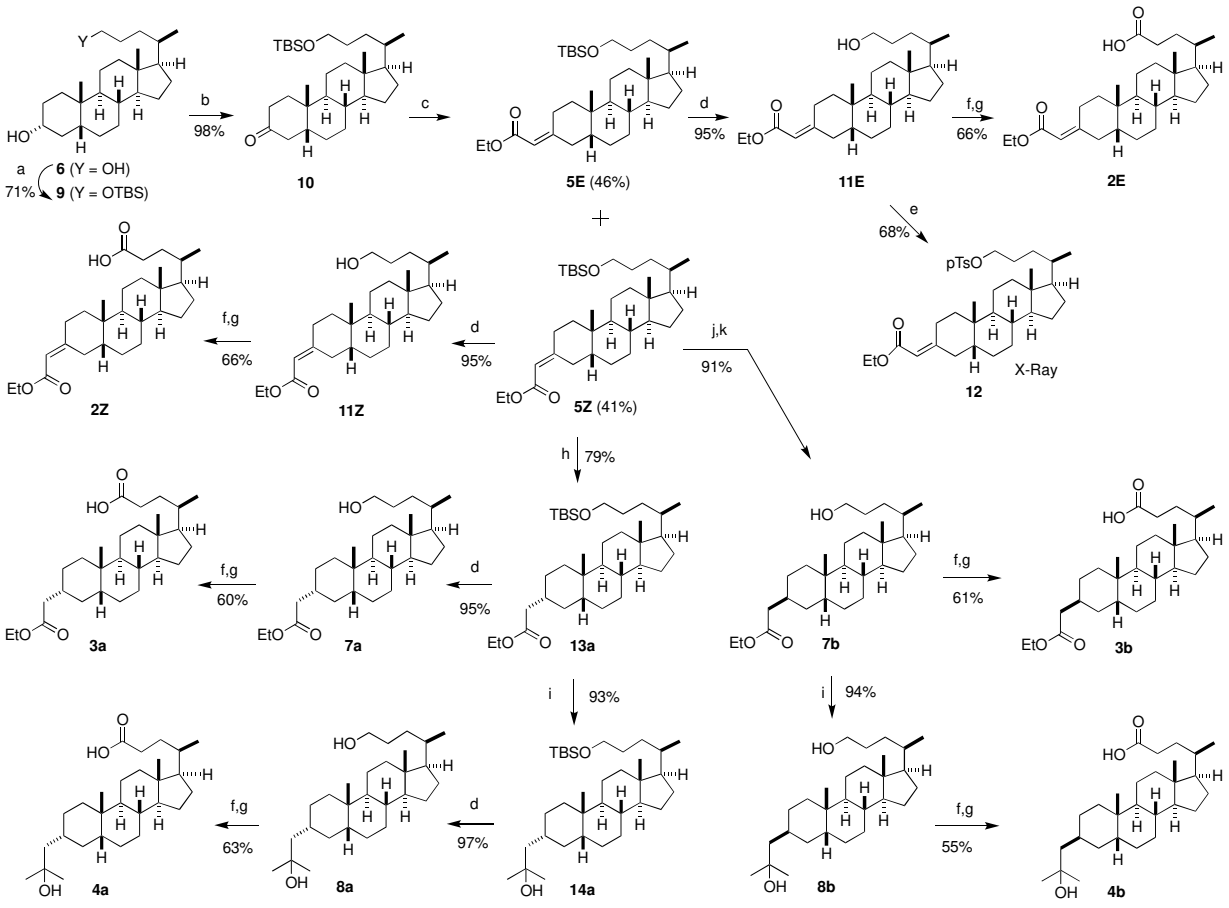

Scheme 2. Synthesis of **2E**, **2Z**, **3a**, **3b, 4a**, and **4b.** [a]**Reagents and conditions**: (a) TBSCl (1 equiv), DMF/CH_2Cl_2; (b) PDC (3 equiv), CH_2Cl_2, 23 ºC, 7 h; (c) $(EtO)_2P(O)CH_2COOEt$ (2 equiv), NaH (2 equiv), THF, 0 ºC, 30 min, then **10**, 23 ºC, 20 min. (d) TBAF (1.5 equiv), THF, 23 ºC, 12 h. (e) *p*-TsCl, pyridine, 0 ºC, 12 h. 0 ºC, 12 h. (f) PDC (3 equiv), CH_2Cl_2, 23 ºC, 12 h. (g Oxone® (1 equiv), DMF, 23 ºC, 3 h. (h) H_2/Pd-C, EtOAc, 23 ºC, 12 h. (i) MeMgBr, THF, 23 ºC, 15 min. (j) PMHS (16 equiv), KO*t*-Bu (0.75 equiv), CuCl (0.7 equiv), (*S*)-tol-BINAP (0.12 equiv), *i*-PrOH, hexanes, -20 ºC to 23 ºC, 3.5 h; (k) HF (48%), THF.

The synthesis of the target compounds **2**-**4** commenced with the known diol **6** [42], which was selectively protected to known alcohol **9** [42] in 71% yield by a modified procedure using *tert*-butyldimethylsilyl chloride (1 equiv) in DMF-CH_2Cl_2. Oxidation of **9** with pyridinium dichromate in CH_2Cl_2 provided ketone **10** in 98% yield. Wadsworth-Horner-Emmons reaction on **9** utilizing the phosphonate anion, prepared from triethyl phosphonoacetate and sodium hydride in THF, afforded, after flash chromatography, a ~1:1 mixture of esters **5E** and **5Z** (96% yield), which could be separated by HPLC (**5E**: 46%, **5Z**: 41%). The structures assigned to **5E** and **5Z** were based on the X-ray analysis of tosylate **12**, prepared in 64% yield by desilylation-tosylation of **5E**. Deprotection of **5E** with *n*-tetrabutylammonim fluoride in THF gave alcohol **11E** in 95% yield, which upon pyridinium dichromate oxidation in CH_2Cl_2 and subsequent treatment of the resulting aldehyde with Oxone® in DMF provided the desired target compound **2E** in 66% (20% yield from **6**, 6 steps). In a similar way, the unsaturated ester **5Z** was converted to target compound **2Z** in 18% yield from **6** (6 steps). The unsaturated ester **5Z** was chosen for the preparation of target compounds **3a**, **3b**, **4a,** and **4b**. Pd-catalyzed hydrogenation of **5Z** in EtOAc furnished a 5:1 mixture of esters (3*R*)-**13a** and (3*S*)-**13b** (95% yield), which were separated by MPLC [silica VersaPak cartridges (1% EtOAc/hexanes)]. Alternatively, ester **13a** could be prepared in similar yield by Pd-catalyzed hydrogenation of **5E** or a ~1:1 mixture of esters **5E** and **7Z**. Ester **13a** was transformed into the target compound **3a** by desilyation-oxidation as above (13%, 7 steps). Methylation of **13a** with methylmagnesium bromide in THF afforded alcohol **14a** (93%), which upon desilylation furnished diol **8a** (98%). Two steps-oxidation of **8a** as above, provided the desired compound **4a** [43] in 63% yield (13% yield from **6**, 8 steps). Diastereoselective reduction of ester **5Z** from the most hindered face with catalytic CuH species [44], generated from catalytic CuCl and excess of PMHS (polymethylhydrosiloxane) as the SiH source, in the presence of *i*-PrOH as the proton source and *tol*-BINAP as the catalytic chiral ligand and catalytic KO*t*-Bu in hexanes, afforded, after desilylation with *n*-tetrabutylammonium fluoride in THF, the ester (3*S*)-**7b** as the only isolated product in 91% yield (two steps). Ester **7b** was converted to target compound **3b** by the two-step oxidation sequence in 61% yield (16% yield from **6**, 6 steps). Methylation of hydroxyester **7b** with methylmagnesium bromide in THF gave diol **8b** (94%), which upon the two-step oxidation sequence as above provided the target compound **4b** in 55% yield (8 steps from **6**).

2.3. Biological evaluation

2.3.1. Binding of the compounds to full length VDR

The affinity of the compounds for VDR was checked using a wide range of concentrations and compared to that of 1,25D. Concentration-response curves were plotted (Fig. 4), and IC50 values were calculated. The binding affinity of each compound was compared to 1,25D, for which the RBA was determined as 100%, and is presented in Table 1. All compounds bind to hVDR with lower affinity compared to 1,25D. In agreement with the docking data, **4a** exhibits the highest affinity being about 15 times lower than 1,25D. For compound **4b** it was about 65 times lower and for compound **2Z** it was about 145 times lower (Table 1). For compounds **3a**, **3b** and **2E** it was not possible to calculate the affinity for the VDR using this assay.

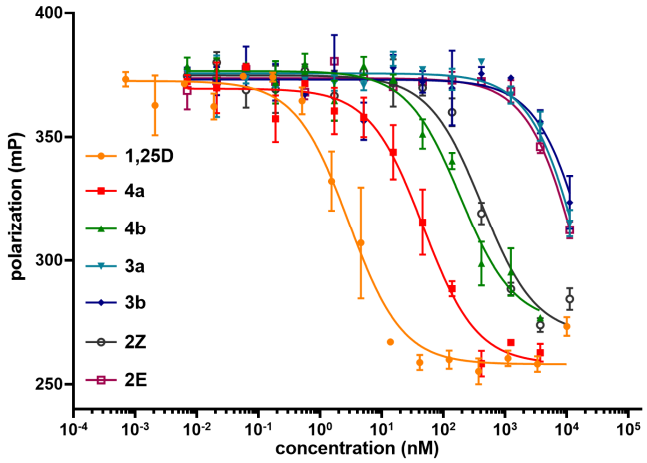

Fig. 4. Concentration-response curves of the affinity of the compounds to VDR. The equilibrium dissociation constants of unlabeled tested compounds were determined by measuring their competition for fluorescent 1,25D bound to recombinant VDR. The change in fluorescence polarization was measured. Three independent experiments were performed, and in every experiment each measurement was done in triplicate. Points on the graph represent means (±SEM) of all measurements. The nonlinear regression curves were fitted to the obtained means using GraphPad Prism 7 software for a one-site binding model.

Table 1. Affinities of the compounds to the recombinant VDR[a]

Compound	**1,25**	**4a**	**4b**	**3a**	**3b**	**2E**	**2Z**
IC_{50} (nM)	2.92	46.53	188.5	ND	ND	ND	424
95% CI	2.036 to 4.182	30.16 to 70.7	117.7 to 301.8	-	-	-	279.7 to 643.4
RBA[b]	100	6.27	1.55	-	-	-	0.69

[a]The VDR binding affinity is expressed as IC_{50} and percentage activity. 95% confidence interval (95% CI) indicates how precisely Prism software has found the best-fit value of an IC_{50}. [b]The potency of 1,25D is normalized to 100. RBA: relative binding affinity. ND: not detected.

2.3.2. Differentiation of HL60 cells

HL60 cells were used to determine pro-differentiating activities of studied compounds. After initial screening the concentration ranges were established for each compound. 1,25D was tested at concentrations 0.032 nM – 100 nM. Compounds **4a**, **4b** and **2Z** were tested at concentrations 0.032 nM – 500 nM, while **3a**, **3b** and **2E** were applied at concentrations 4 µM – 50 µM. The cells were exposed to the compounds for 96 h and then the expression of monocyte/macrophage differentiation marker CD14 [46] was studied using flow cytometry.

Percentages of CD14-positive cells were read out using Becton Dickinson Accuri C6 software. Results are presented in Figure 5. EC50 values were estimated from dose-response curves using GraphPad Prism 7 software. Effective molar ratios (EMR) for each compound in comparison to 1,25D for CD14 antigen are presented in Table 2.

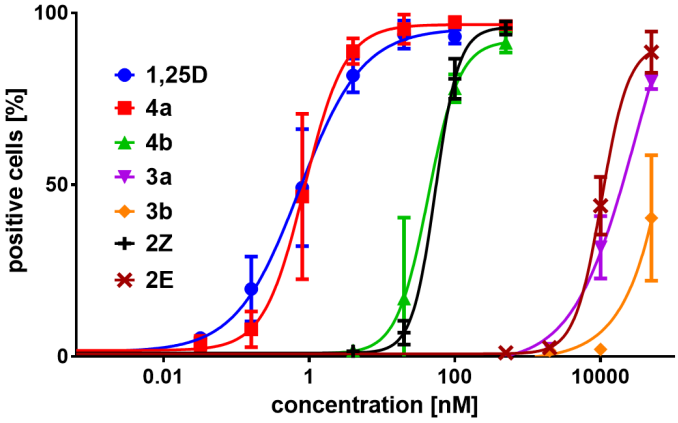

Fig. 5. Concentration-response curves of CD14-positive cells induced by 1,25D or studied compounds. HL60 cells were exposed to 1,25D or to the compounds at wide range of concentrations for 96 h. Then the expressions of CD14 cell surface marker were detected by flow cytometry. Mean values (±SEM) of percentages of antigen-positive cells are presented. Compounds **4a**, **4b** and **2Z** were tested at concentrations of 0.032 nM – 500 nM, while **3a**, **3b** and **2E** were applied at concentrations of 4 µM – 50 µM. Percentages of CD14-positive cells were read out using Becton Dickinson Accuri C6 software. EC_{50} values were estimated from concentration-response curves fitted to the obtained means using GraphPad Prism 7 software.

Table 2. Induction of CD14-positive cells by 1,25D and the compounds.

Compound	**1,25**	**4a**	**4b**	**3a**	**3b**	**2E**	**2Z**
IC_{50} (nM)	0.731	0.859	42.79	31 279	ND	10 363	54.04
95% CI	0.4728 to 1.13	0.6564 to 1.124	29.24 to 62.63	17 593 to 55 614	-	9 008 to 11 922	47.44 to 61.56
EMR[a]	1	0.85	0.017	0.00002	-	0.00007	0.014

EC_{50} values were estimated from concentration-response curves using GraphPad Prism 7 software. 95% confidence interval (95% CI) indicates how precisely Prism software has found the best-fit value of an EC_{50}. The EC_{50} values were used to calculate the effective molar ratio (EMR). [a]EMR = EC_{50} 1,25D/EC_{50} compound: ND: not determined.

2.3.3. Nuclear translocation and accumulation of VDR in response to the tested compounds

Given that VDR nuclear accumulation and pro-differentiating activity were correlated for previously tested analogs [47], we studied how the compounds influence the levels of VDR protein in HL60 cells exposed for 24 h to analogs at 100 nM concentration. We analyzed VDR levels in nuclear fractions of cells. Nuclear protein HDAC2 was used as a control, as this protein does not change during HL60 cell differentiation. The amount of VDR in the cell nuclei increased in the cells exposed to 1,25D and compounds **4a**, **4b** and **2Z** (Fig. 6).

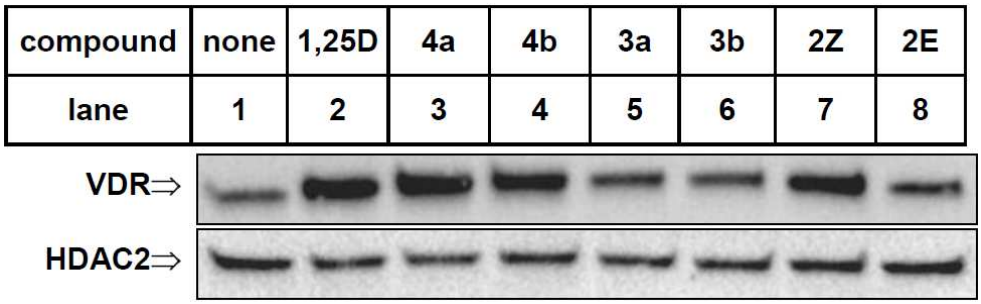

Fig. 6. Nuclear localization of VDR protein in HL60 exposed to 1,25D or studied compounds. HL60 cells were treated for 24 h with 100 nM 1,25D or 100 nM compounds. Nuclear extracts were separated in SDS-PAGE and electro-blotted to PVDF membrane. The membrane was probed against VDR and HDAC2.

2.3.4. Expression of CYP24A1 and CD14 in HL60 cells in response to 1,25D and to the tested compounds

Encouraged by the above results and to further determine whether the compounds activate VDR in HL60 cells, we evaluated the ability of the compounds to stimulate VDR activity by measuring *CYP24A1* and *CD14* transcript levels in HL60 cells. For analysis of *CYP24A1* expression, cells were treated with 1,25D or the compounds at 10 nM and 100 nM concentrations for 96 h (Fig. 7a-b). Out of the tested compounds, only **4a** induced *CYP24A1* transcript level with similar potency as 1,25D. For *CD14* transcript levels, HL60 cells were treated with 1nM, 10nM and 100nM 1,25D or the compounds (Fig. 7c-e). Again, **4a** was the most potent analog to induce the expression of *CD14*, while **4b** and **2Z** only weakly stimulated the expression of *CD14* target gene. At 10 nM concentration **4a** was significantly stronger than 1,25D in activating expression of *CD14* gene in the same cells (Fig. 7d).

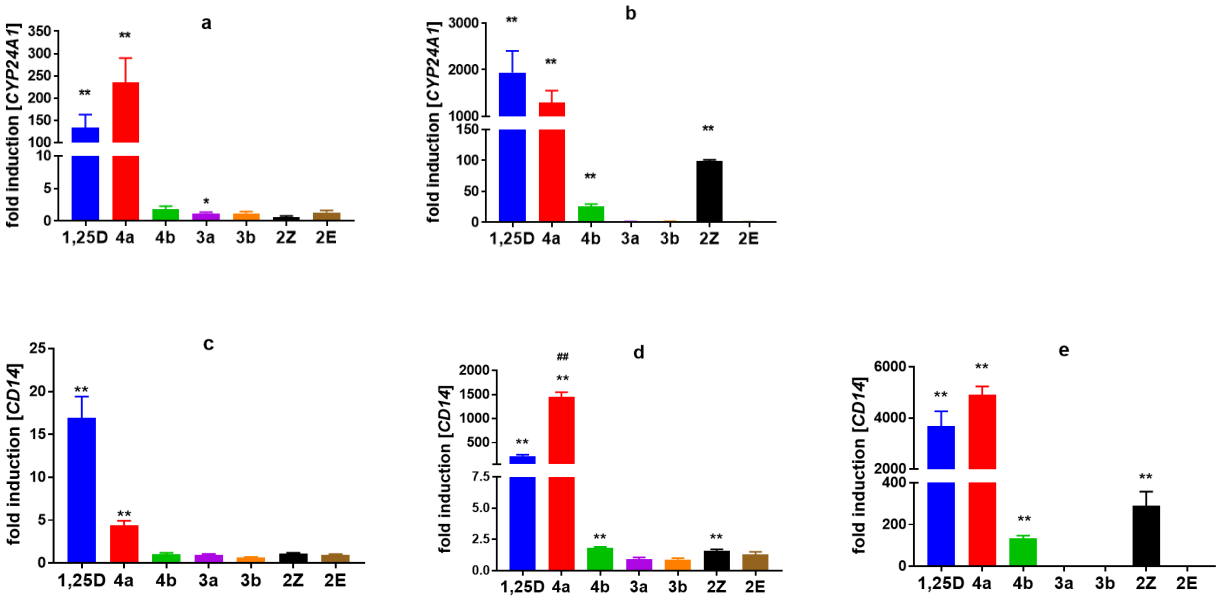

Fig. 7. Expression of *CYP24A1* and *CD14* in HL60 cells exposed to 1,25D or to the tested compounds. HL60 cells were exposed to 1,25D or tested compounds, and after 96 h the expression of *CYP24A1* or *CD14* mRNA was measured by Real time PCR. The expression of *CYP24A1* in the cells exposed to the 10 nM (a) or 100 nM (b) compounds and the expression of *CD14* mRNA in the cells exposed to 1 nM (c), 10 nM (d) or 100 nM (e) compounds. Control cells were treated with equivalent volume of ethanol (solvent for the above compounds). The bar charts show the mean values (±SEM) of the fold inductions in mRNA levels relative to *GAPDH* mRNA levels. Values that are significantly higher than those obtained for respective control cells are marked with asterisks (*p < 0.05; **p<0.01). The expression which was significantly higher than in cells treated with 1,25D is marked with a hashtag (##p<0.01).

2.3.5. Expression of *TRPV6* in HT-29 cells in response to 1,25D and to the tested compounds

In addition, *TRPV6* transcript levels in cells derived from colon cancer (HT-29) were also analyzed. One of the main actions of 1,25D is to ensure intestinal calcium and phosphate absorption. *TRPV6*, located at the brush border membranes of intestinal cells, is a potential mediator of calcium uptake from the diet [48]. The gene encoding this calcium channel is directly regulated by 1,25D by activating multiple vitamin D receptor binding sites [49]. Cells were treated with 1,25D or tested compounds at 10 nM and 100 nM concentrations for 96 h. Interestingly in HT-29 cells, **4a** was significantly more effective than 1,25D in activating expression of *TRPV6* gene (Fig. 8).

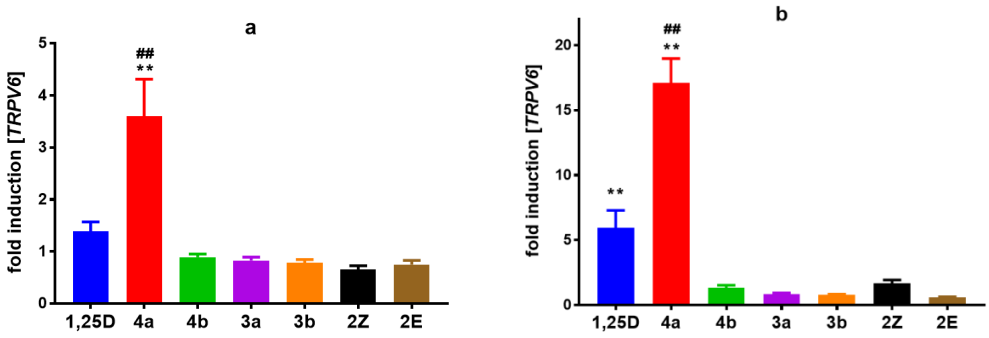

Fig. 8. Expression of *TRPV6* in HT-29 cells induced by 1,25D or tested compounds. HT-29 cells were exposed to 10 nM (a) or 100 nM (b) 1,25D or tested compounds and after 96 h the expression of *TRPV6* mRNA was measured by Real time PCR. The bar charts show the mean values (±SEM) of the fold induction in mRNA levels relative to *GAPDH* mRNA levels. Values that are significantly higher than those obtained for respective control cells are marked with asterisks **p<0.01). The expressions which were significantly higher than in cells treated with 1,25D are marked with hashtags (##p<0.01).

2.3.6. Calcemic activity of compound 4a

The calcemic activity of the most potent compound, **4a**, was evaluated by the analysis of serum calcium concentrations after 7 days of intraperitoneal administration of different dosages of either 1,25D (daily doses of 0.08; 0.16; or 0.32 µg/kg/d), compound **4a** (daily doses of 0.1; 0.2; or 0.4 µg/kg/d) or vehicle (arachis oil). Compound **4a** was about 5-fold less calcemic than the parent molecule 1,25D, as a 5-fold higher dose of **4a** could be administered before a significant increase in serum calcium was observed (Fig. 9).

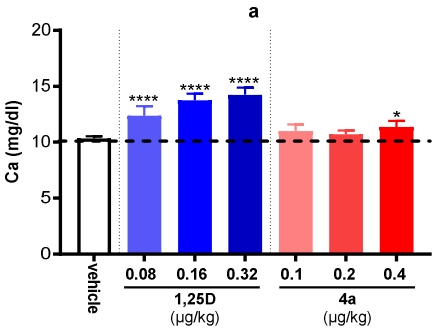

Fig. 9. Calcemic activity of compound **4a**. Mice were injected with vehicle (arachis oil), different doses of 1,25D or compound **4a**. Serum calcium levels were significantly higher in all 1,25D-treated groups than in vehicle-treated mice (****p<0.0001, one way ANOVA followed by Dunnett's multiple comparisons test). Serum calcium levels were only slightly elevated in the group treated with the highest dose of compound **4a** when compared to vehicle-treated mice (*<p0.05, one way ANOVA followed by Dunnett's multiple comparisons test).

2.4. Crystal structure of VDR-4a

The binding mode of **4a** compound into zVDR LBD was determined by X-ray crystallography (Fig. 10a). In contrast to parental **1a** molecule bound to zVDR LBD, only one molecule of **4a** was found bound to the canonical

ligand binding pocket, as reported by Sasaki et al using the rVDR LBD [39]. Similarly to previous structures of VDR complexes with LCA and its derivatives, **4a** adopts an orientation opposite to that of 1,25D (Fig. 9c). Superposition of the VDR LBP in the presence of **4a** and **1a** shows similar positioning of the ligands, in agreement with the docking results. The carboxy group of **4a** forms direct hydrogen bonds to zTyr175(hTyr143) and zSer306(hSer278) and water-mediated hydrogen bonds to zSer265 (hSer237) and zArg302(hArg274) and the hydroxyl group of the 3-hydroxyethyl forms direct hydrogen bonds with zHis333(hHis305) and zHis423(hHis397) (Fig. 9b) similarly to the 25-hydroxyl group of 1,25D, that form hydrogen bonds with the two histidines. In contrast the carbonyl oxygen of **1a** forms a single water-mediated hydrogen bond with zHis423(hHis397). The A, B, C and D rings of 4a form identical interactions with VDR LBP residues as **1a**. The longer length of **4a** (15.8 Å) compared to **1a** (14 Å) allows **4a** to form additional interactions (Fig. 9b) with zLeu255(hLeu227) in helix H3 at 3.6 Å, zTyr427(hTyr401) in helix H11 at 4.1 Å and zVal444(hVal418) in helix H12 at 3.7 Å, compared to 1a. In contrast to **1a** that does not stabilize the C-terminal part of VDR, **4a** stabilizes the agonist conformation of VDR complex, explaining the high potency of **4a** to activate VDR-mediated transcription.

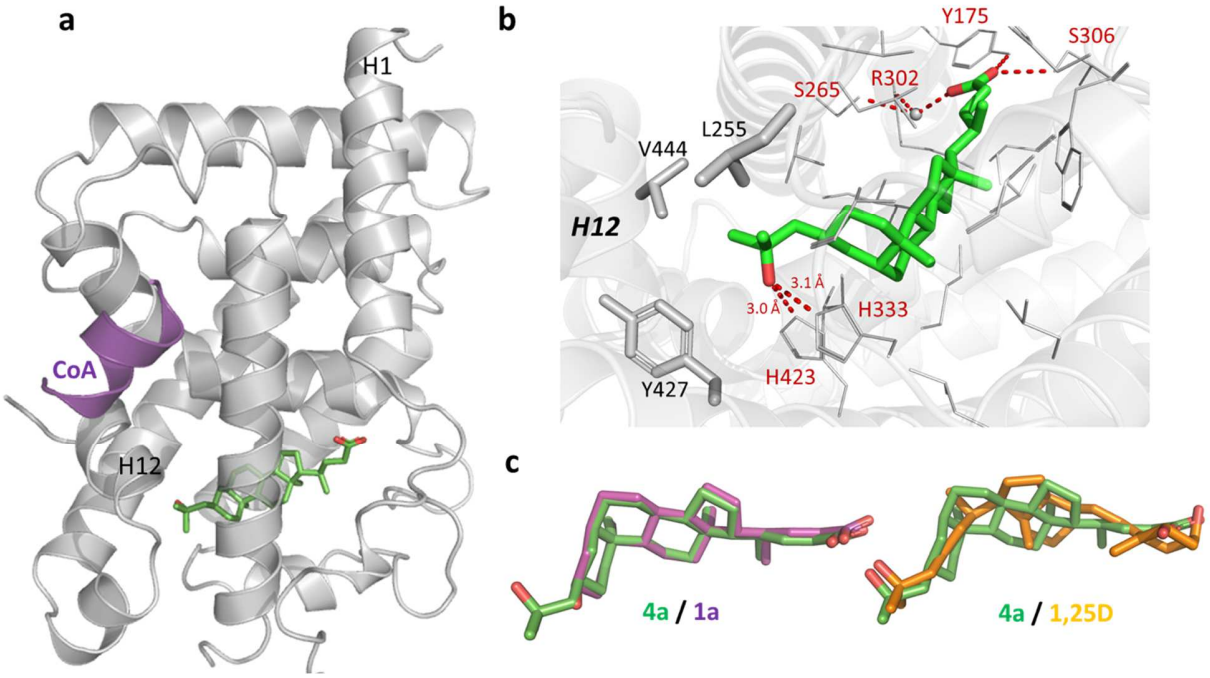

Fig. 9. Crystal structure of VDR-**4a**. (a) Overall structure of the zVDR LBD-**4a** complex. (b) Details of interactions of 4a with residues of the VDR binding pocket at a 4.0 Å distance cutoff. Hydrogen bonds are shown as red dashed lines and water molecule as sphere. Additional interactions compared to **1a** are shown in stick representation and labelled. (c) Superposition of **4a** (green) and **1a** (purple) or 1,25D (orange) molecules in the canonical VDR binding pocket.

2.5. Conclusions

Six lithocholic derivatives were designed in silico using the crystallographic structure of the VDR LBD. The new LCA derivatives **2E**, **2Z**, **3a**, **3b**, and known **4a**, and **4b** were stereoselectively synthetized through an efficient linear route starting from lithocholic acid. Our synthetic route, as for **4a**, does not use compound mixtures, is more direct, and is more efficient (8 steps, 24% overall yield) than the previously reported one (16 steps, 4%

yield) [38]. The HL60 cell differentiation measured by the acquisition of CD14 cell surface marker was comparable for 1,25D and compound **4a**. Compounds **4b** and **2Z** needed to be applied at concentrations two orders of magnitude higher than 1,25D to reach similar cell-differentiating effect. Compounds **3a** and **3b** were four orders of magnitude less potent than 1,25D in this assay, and the compound **2E** showed only trace activity. Compounds **4a**, **4b** and **2Z** induced accumulation of VDR protein in the nuclei of HL60 cells similarly to 1,25D. In addition, the results obtained in real-time PCR assays indicated that the ability to induce transcription of VDR target genes was dependent on the target gene, on the concentration of the compound and depending of the cell types. Compound **4a** showed similar potency than 1,25D in activating expression of *CYP24A1* gene in HL60 cells. However, at 10 nM concentration **4a** was significantly stronger than 1,25D in activating expression of CD14 gene in the same cells. In HT-29 cells, **4a** was significantly more effective than 1,25D in activating expression of TRPV6 gene. Out of the six new compounds tested, the compound **4a** was the most active in biological tests in accordance with reported assays [38]. Interestingly, compound **4a** was about 5-fold less calcemic than 1,25D when evaluated after intraperitoneal injections in mice, making it of potential therapeutic value.

3. Materials and methods

3.1. Docking procedure

The proposed LCA ligands were built, using the three-dimensional structure of 1,25D, obtained from the crystallographic structure of 1,25 D in complex with hVDR (PDB code: 1DB1) [29]. Modifications to the ligands were carried out with the builder mode of Pymol and the editing tool provided by the Chem3D software. Docking studies to predict the affinity of each ligand for the VDR LBD were made using the Gold software (version Suite 5.4). A modified structure of VDR LBD, with inclusion of hydrogens and missing gap regions, was used as the protein. The binding site of the protein was set automatically with a 6 Å radius. Docking was performed in 25 independent genetic algorithm (GA) runs. In each run, a maximum of 125000 GA operations were performed in a single population of 100 individuals. Default parameters were employed for hydrogen bonds (4.0 Å) and Van der Waals interactions (2.5 Å). ChemPLP was used as the scoring function and GoldScore was used as the re-scoring function. For each ligand, the three best solutions were normalized using the score of 1,25D as the reference value (100%).

3.2. Synthesis

General procedures. All reactions involving oxygen- or moisture-sensitive compounds were carried out under a dry Ar atmosphere using oven-dried or flame-dried glassware and standard syringe/septa techniques, unless when indicated. Liquid reagents or solutions of reagents were added by syringe or cannula techniques. Reaction temperatures refer to external bath temperatures. Acetone–dry ice baths were used for reactions at low temperature. Alternatively, methanol or acetone baths were cooled with a CRYOCOOL immersion cooler, provided with a temperature regulator. Organic extracts were dried over anhydrous Na_2SO_4, filtered and concentrated using a rotary evaporator at aspirator pressure (20-30 mm Hg). Reagents were obtained from Aldrich Chemical (www.sigma-aldrich.com) or Acros Organics (www.acros.com) and used without further

purification. All dry solvents were distilled under Ar immediately prior to use. Tetrahydrofuran (THF) and Et_2O were distilled from Na/benzophenone. CH_2Cl_2 was distilled from P_2O_5. DMF was dried over molecular sieve 4Å. *tert*-Butyl methyl ether (TBME) and CH_2Cl_2 for extractions were used as received. Reactions were monitored by thin-layer chromatography (TLC) using aluminum-backed MERCK 60 silica gel plates (0.2 mm thickness). The chromatograms were visualized first with ultraviolet light (254 nm) and then by immersion in solutions of ceric ammonium molybdate or *p*-anisaldehyde followed by heating with a heater gun. Flash column chromatography was performed with Merck silica gel 60 (230-400 mesh). NMR spectra were measured with solutions in $CDCl_3$ in a Bruker DPX-250 or Bruker AMX-500 spectrometers. Chemical shifts are reported on the δ scale (ppm) downfield from tetramethylsilane (δ 0.0 ppm) using the residual solvent signal at δ = 7.26 ppm (^{1}H, s, $CDCl_3$) or δ 77.0 ppm (^{13}C, t, $CDCl_3$). Coupling constants (*J*) are reported in Hz. Distortionless Enhancement by Polarization Transfer (DEPT-135) was used to assign carbon types. NMR signals have been assigned using steroidal numbering. High resolution mass spectra (HRMS) were performed in a Micromass Instruments Autospec, a Thermo Finningan MAT95XP and an Applied Biosystems QSTAR Elite spectrometers. IR spectra were recorded on a silicon disc on a Bruker IFS-66V and VECTOR 22 FT-IR spectrometers. UV spectra were registered in a Hewlett Packard 8452A spectrometer. Optical rotations were measured on a Jasco DIP-370 polarimeter in a 1 dm cell. [α] and *c* are given in deg $cm^3g^{-1}dm^{-1}$ and g cm^{-3} respectively.

Target compounds **2E** and **2Z** were purified by HPLC [Shimadzu preparative liquid chromatograph, model LC-8A equipped with a UV-1 absorbance detector using a phenomenex luna, silica, 5µ, 250x21 mm column and 30% EtOAc/hexanes as eluent (Flow rate: 3 mL/min) (see SI)]. Target compounds **3a**, **3b**, **4a** and **4b** were purified by HPLC as per **2E** and **2Z,** replacing the absorbance detector by TLC monitoring.

(3α,5β)-24-[(*tert*-Butyldimethylsilyl)]oxy-cholan-3-ol (9).
A mixture of diol **6** (6.8 g, 18.75 mmol), imidazole (1.276 g, 18.74 mmol), and dry DMF (150 mL) was stirred for 30 min. Dry CH_2Cl_2 (20 mL) was added. The mixture was stirred for 30 min. A solution of TBSCl (2.81 g, 18.75 mmol) in dry CH_2Cl_2 (20 mL) was added via syringe pump (20 mL syringe, flow rate = 5 mL/h, 2.30 h). The CH_2Cl_2 was removed in vacuo. Saturated NaCl (300 mL) was added. The mixture was extracted with EOAc (2x100 mL). The solid starting diol was removed by filtration. The combined organic extracts were concentrated and redissolved in a small volume of EtOAc by heating. The resulting solution was flash chromatographed (SiO_2, 5x15 cm, 5-20% EtOAc/hexanes) to give the diprotected diol (0.976 g, 9%, 5% EtOAc/hexanes) and **9** [6.35 g, 71%, white solid, R_f = 0.5 (20% EtOAc/hexanes)] [42]. $[\alpha]_D^{25}$ = +40.2 (c 0.5, $CHCl_3$)]. **^{1}H NMR** (250 MHz, $CDCl_3$) δ 3.5-3.7 (m, 3H), 1.3-1 (m, 12H), 0.90 (d, s, 12H), 0.63 (s, 3H), 0.04 (s, 6H). **^{13}C NMR** (63 MHz, $CDCl_3$) δ 71.7 (CH), 63.7 (CH_2), 56.35 (CH), 56.0 (CH), 42.5 (CH), 41.9 (CH), 40.3 (CH_2), 40.0 (CH_2), 36.3 (CH), 35.7 (C), 35.4 (C), 35.2 (CH), 34.4 (CH), 31.7 (CH_2), 30.4 (CH_2), 29.3 (CH_2), 28.1 (CH_2), 27.06 (CH_2), 26.3 (CH_2), 25.8 (CH_2), 24.1 (CH_2), 23.24 (3xCH_3), 20.7 (CH_3), 18.5 (CH_2), 18.2 (CH_3), 11.89 (CH_3), -5.37 (2xCH_3).

5β,24-[(*tert*-Butyldimethylsilyl)oxy]-cholan-3-one (10). Pyridinium dichromate (2.60 g, 6.93, 3 equiv) was added to a solution of (3α,5β)-24-[(*tert*-butyldimethylsilyl)]oxy-cholan-3-ol (**9**, 1.10 g, 2.31 mmol) in dry CH_2Cl_2 (45 mL). The mixture was stirred in the dark at 23 ºC for 7 h. The resulting black mixture was diluted with TBME (50 mL) and filtered through a pad of Celite/silicagel washing the solids with TBME (3x20 mL). The solution was

concentrated and the white solid was purified by flash chromatography (SiO_2, Ø 2.5x5 cm, 2% EtOAc/hexanes) to afford **10** [1.02 g, 2.14 mmol, 98%, white solid (mp 69-69.5 ºC) R_f = 0.75 (20% EtOAc/hexanes)]. **^{1}H NMR** (250 MHz, $CDCl_3$) δ 3.5 (t, *J* = 5.8 Hz, 2H), 2.7-2.2 (m, 4H), 1.0 (s, 3H), 0.9 (d,s, 12H), 0.65 (s, 3H), 0.02 (s, 6H). **^{13}C NMR** (63 MHz, $CDCl_3$) δ 213.4 (CO), 63.7 (CH_2), 56.4 (CH), 56.1 (CH), 44.3 (CH), 42.6 (C), 42.3 (CH_2), 40.6 (CH), 40.0 (CH_2), 37.16 (CH_2), 36.9 (CH), 35.4 (C), 34.8 (C), 31.8 (CH_2), 29.3 (CH_2), 28.1 (CH_2), 26.5 (CH_2), 25.9 (C), 25.7 (CH_2), 24.1 (CH_2), 22.6 (3xCH_3), 21.1 (CH_2), 18.6 (CH_3), 18.3 (CH_3), 12.0 (CH_3), -5.3 (2xCH_3). **IR** (film, cm^{-1}): 1715 (CO). **HRMS** (**EI**): calcd for $C_{30}H_{55}O_2Si$ $[M+H]^+$, 476.3971; found, 476.3968.

(*E*)-3-(2-Ethoxy-2-oxoethylidene)-5β-cholan-24-ol *tert*-Butyldimethylsilyl Ether (5E) and (Z)-3-(2-Ethoxy-2-oxoethylidene)- 5β-cholan-24-ol tert-Butyldimethylsilyl Ether (5Z). Triethyl phosphonoacetate (6.91 g, 30.83 mmol, 6.14 mL, 2 equiv) was added dropwise to a 0 ºC cooled suspension of NaH [0.74 g, 30.83 mmol, (1.24 g, 60% w/w)] in dry THF (20 mL). The mixture was stirred for 30 min. A solution of ketone **9** (6.13 g, 12.92 mmol) in dry THF (10 mL) was added via cannula. The cooling bath was removed and the reaction mixture was stirred for 20 min. The reaction was quenched by successive addition of drops of H_2O and H_2O (20 mL). The mixture was concentrated to a small volume. TBME (100 mL) and H_2O (100 mL) were added. The aqueous phase was extracted with TBME. The combine organic extracts were concentrated in *vacuo* and the residue was purified by flash chromatography (SiO_2, Ø 4x7 cm, 2% EtOAc/hexanes) to give a 1:1 mixture of **5Z** and **5E** [6.8 g, 96%, colorless oil, *Rf* = 0.72 (15% EtOAc/hexanes)]. A fraction of this mixture (1.43 g) was chromatographed by HPLC (Phenomenex Luna, silica, 5µ, 250x21 mm, 0.2 % EtOAc/hexanes, flow rate: 13 mL/min) to give **5E** [0.65 g, 46%, retention time: 38 min, $[\alpha]_D^{25}$ +24.5 (c 0.4, $CHCl_3$)] and **5Z** [0.55 g, 41%, retention time: 43 min, $[\alpha]_D^{25}$ +41.5 (c 0.4, $CHCl_3$)]. **5E: ^{1}H NMR** (250 MHz, $CDCl_3$) δ 5.55 (s, 1H), 4.1 (q, *J* = 7.1 Hz, 2H), 3.5 (t, *J* = 6.4 Hz, 2H), 1.2 (m, 10H), 0.9 (d, s, 12H), 0.62 (s, 3H), 0.00 (s, 6H). **^{13}C NMR** (63 MHz, $CDCl_3$) δ 166.8 (C=O), 164.8 (C3), 112.5 (CH=), 63.6 (O**C**H_2CH_3), 59.2 (OCH_2), 56.4 (CH), 56.0 (CH), 44.7 (CH), 42.5 (C), 40.5 (CH_2), 40.0 (CH_2), 38.45 (CH), 35.6 (CH_2), 35.4 (CH_2), 35.1 (CH_2), 32.65 (CH_2), 31.7 (CH_2), 30.15 (CH_2), 29.6 (C), 29.25 (CH_2), 28.09 (CH_2), 27.0 (CH_2), 26.0 (CH_2), 25.82 (3xCH_3), 24.05 (CH_2), 23.2, 20.95 (CH_2), 18.5 (CH), 18.2 (C), 14.17 (CH_3), 11.91 (CH_3), -5.40 (2xCH_3). **IR** (film, cm^{-1}): 2929, 2858, 1715, 1647. **HRMS** (EI): calcd for $C_{34}H_{61}O_3Si$ $[M+H]^+$, 545.4389; found, 545.4384. **5Z**: This compound can be distinguished from its **5E** isomer by **^{13}C NMR** (DEPT) at δ 45.5. **IR** (film, cm^{-1}) as for **5E**. **HRMS** (EI): calcd for $C_{34}H_{61}O_3Si$ $[M+H]^+$, 545.4389; found, 545.4384.

(*E*)-3-(2-Ethoxy-2-oxoethylidene)-5β-cholan-24-ol (11E). A solution of TBAF in THF (1.1 mL, 1.1 mmol, 1M, 1.5 equiv) was added to a solution of **5E** (0.400 g, 0.740 mmol, 1 equiv) in THF (10 mL). The reaction mixture was stirred at 23 °C for 12 h. The reaction was quenched with saturated NaCl. The mixture was extracted with EtOAc (3x7 mL). The combined organic extracts were dried, filtered and concentrated. The residue was purified by flash chromatography (SiO_2, Ø 1.5×6 cm, 12% EtOAc/hexanes) to give **11E** [0.301 g, 95%, *Rf* = 0.25 (20% EtOAc/hexanes), white solid (mp 85-87 °C)]. $[\alpha]_D^{25}$ +35.5 (*c* 1.2, $CHCl_3$). **^{1}H NMR** (250 MHz, $CDCl_3$) δ 5.55 (s, CH=, 1H), 4.1 (dt, *J* = 7.1 Hz, C(O)OCH_2, 2H), 3.9 (t, *J* = 6.1 Hz, OCH_2, 2H), 2.6 (m, 1H), 1.2 (t, *J* = 7.1, Hz, 3H), 0.9 (s, d, 6H), 0.6 (s, 3H). **^{13}C NMR** (63 MHz, $CDCl_3$) δ 166.7 (CO), 164.9 (CO), 112.4 (CH=), 63.4 (CH_2), 59.3 (CH_2), 56.3 (CH), 56.0 (C), 45.5 (CH), 42.55 (CH), 40.4 (C), 40.0 (CH_2), 38.1 (CH_2), 37.9 CH_2), 35.5 (C), 35.4 (C), 35.1 (CH), 31.7 CH_2), 29.2 (CH_2), 28.2 (CH_2), 26.8 (CH_2), 26.0 (CH_2), 24.6 (CH_2), 24.05 (CH_2), 23.0 (CH_3), 20.9 (CH_2), 18.5 (CH_2), 14.2 (CH_2), 11.9 (CH_2). **IR** (film, cm^{-1}): 3412, 2931, 2864, 1711, 1647. **HRMS** (EI): calcd for $C_{28}H_{47}O_3$ $[M+H]^+$, 431.3525; found, 431.3520.

(*E*)-3-(2-Ethoxy-2-oxoethylidene)-5β-cholan-24-ol *p*-Toluenesulfonate (12). A solution of alcohol **11E** (0.122 g, 0.28 mmol) and *p*-TsCl (0,08 g, 1.5 equiv) in dry pyridine (2 mL) was allowed to stand at 0 ºC overnight. The mixture was poured onto saturated $CuSO_4$ and extracted with CH_2Cl_2. The organic phase was washed with saturated $CuSO_4$, dried, filtered and concentrated. The residue was purified by flash chromatography (SiO_2, Ø 1.5×3 cm, 2% EtOAc/hexanes) to afford **12** [0.164 g, 68%, white-pink solid (mp 114-114.5 ºC), *Rf* = 0.75 (20% EtOAc/hexanes)]. IR (film, cm-1): 2925, 2857, 1713, 1647, 1447, 1363, 1210, 1152. **HRMS** (EI): calcd for $C_{35}H_{53}O_5S$ $[M+H]^+$, 585.3614; found, 585.3527. **^{1}H NMR** (250 MHz, $CDCl_3$) δ 7.34 (d, CH-Ar, *J* = 8.2 Hz, 2H), 7.30 (d, CH-Ar, *J* = 8.2 Hz, 2H) 5.54 (s, =CH, 1H), 4.08 (q, *J* = 7.1 Hz, -C**H$_2$**O), 3.95 (t, *J* = 6.1 Hz, -CH_2O), 2.40 (s, CH_3-Ar), 1.22 (t, *J* = 7.1 Hz, **CH_3**CH_2COO). 0.88 (s, 3H), 0.81 (d, *J = 6.4 Hz*, 3H), 0.58(s, 3H). **^{13}CNMR** (63 MHz, $CDCl_3$) δ 166.64 (C).164.57 (C), 144.42 (C),131.18 (C), 127.71 (CH), 112.44 (CH), 71.06 (CH_2), 59.23 (CH_2), 56.32 (CH), 55.84 (CH), 45.52 (CH), 42.54 (C), 40.42 (CH), 39.97 (CH_2), 38.12 (CH_2), 37.92 (CH_2), 35.55 (CH), 35.03 (CH), 31.27 (CH_2), 28.03 (CH_2), 26.81 (CH_2), 25.39 (CH_2), 24.55 (CH_2), 24.00 (CH_2), 23.01 (CH_3), 21.46 (CH_3), 20.84 (CH_2), 18.25 (CH_3), 14.17 (CH_3), 11.87 (CH_3).

(*Z*)-3-(2-Ethoxy-2-oxoethylidene)-5β-cholan-24-oic Acid (2E*).*** Pyridinium dichromate (0.523 g, 1.29 mmol, 3 equiv) was added to a solution of alcohol **11E** (0.200 g, 0.464 mmol, 1 equiv) in dry CH_2Cl_2 (35 mL). The mixture was stirred in the dark at 23 ºC for 12 h. The resulting black mixture was diluted with TBME (10 mL) and filtered through a pad of Celite/silicagel washing the solids with TBME (3x20 mL). The solution was concentrated to afford the corresponding aldehyde (0.180 g, 90%), which was immediately dissolved in dry DMF (10 mL) and treated with Oxone (0.077 g, 0.509 mmol). The mixture was stirred at room temperature for 3 h. The reaction was quenched with saturated NaCl. The mixture was extracted with EtOAc (3x7 mL). The combined organic extracts were dried, filtered and concentrated and the residue was purified by flash chromatography (SiO_2, Ø 1.5X7 cm, 25% EtOAc/hexanes) to afford **2E** [110 mg, 66%, R_f = 0.20 (30% EtOAc/hexanes), white solid (mp 92-94 °C)]. $[\alpha]_D^{25}$ +46.5 (*c* 1, $CHCl_3$). **^{1}H NMR** (250 MHz, $CDCl_3$) δ 5.55 (s, CH=, 1H), 4.1 (q, OCH_2, *J* = 7.1 Hz, 2H), 2.6 (m, 1H), 2.3 (m, 1H), 1.2 (t, OCH_2**CH_3**, *J* = 7.1 Hz, 3H), 0.9 (s, d, 6H), 0.62 (s, 3H). **^{13}C NMR** (63 MHz, $CDCl_3$) δ 180.2 (CO), 166.7 (CO), 164.7 (C=), 112.4 (CH=), 59.3 (CH_2), 56.3 (CH), 55.8 (CH), 45.5 (CH), 42.6 (C), 40.4 (CH), 40.0 (CH_2), 38.1 (CH_2), 37.9 (CH), 35.6 (CH), 35.1 (CH), 30.9 (CH_2), 30.6 (CH_2), 28.0 (CH_2), 26.8 (CH_2), 26.0 (CH_2), 24.6 (CH_2), 24.0 (CH_2), 23.0 (C), 20.85 (CH_2), 18.1 (CH_3), 14.2 (CH_3), 14.0 (CH_3), 11.9 (CH_3). **IR** (film, cm^{-1}): 3435, 2931, 2864, 1711, 1646. **HRMS** (EI): calcd for $C_{28}H_{44}O_4$ $[M+Na]^+$, 467.3137; found, 467.3132. A sample of **2E** for biological testing was purified by HPLC as indicated in general procedures (see also SI).

(*Z*)-3-(2-Ethoxy-2-oxoethylidene)-5β-cholan-24-ol (11Z). As per **11E. 11Z** [0.301 g, 0.698 mmol 95%, *Rf* = 0.25 (20% EtOAc/hexanes), white solid (mp: 92-94 °C)]. $[\alpha]_D^{25}$ +34.80 (*c* 1, $CHCl_3$). **^{1}H NMR** (250 MHz, $CDCl_3$) δ 5.6 (s, 1H), 4.1 (q, *J* = 7.1 Hz, 2H), 3.6 (t, 2H), 2.37 – 2.03 (m, 2H), 1.4 (t, *J* = 7.1 Hz, 3H), 0.9 (s, d,

6H), 0.61 (s, 3H). **^{13}C NMR** (63 MHz, $CDCl_3$) δ 166.9 (CO), 164.9 (C=), 112.4 (CH=), 63.4 (O**CH_2**CH_3), 59.3 (OCH_2), 56.3 (CH), 56.0 (C), 47 (CH), 42.54 (C), 40.45 (CH), 40.0 (CH_2), 38.42 (CH_2), 35.6 (C, C-10), 35.4 (CH), 35.1 (C), 32.65 (CH_2), 31.65 (CH_2), 30.2 (CH_2), 29.2 (CH_2), 28.15 (CH_2), 27.0 (CH_2), 26.0 (v), 24.04 (CH_2), 23.2 (CH_3), 20.9 (CH_2), 18.5 (CH_3), 14.2 (CH_3), 11.9 CH_3). **IR** (film, cm^{-1}); 3404, 2936, 2863, 1710, 1646. **HRMS** (EI): calcd for $C_{28}H_{46}O_3Na$ $[M+Na]^+$, 453.3345; found 453.3339.

(*Z*)-3-(2-Ethoxy-2-oxoethylidene)-5β-cholan-24-oic Acid (2Z). As per **2E**. **2Z** [137 mg, 66%, R_f = 0.20 (30% EtOAc/hexanes), white semisolid]. $[\alpha]_D^{25}$ +32.1 (c 1, $CHCl_3$). **^{1}H NMR** (250 MHz, $CDCl_3$) δ 5.6 (s, CH=, 1H), 4.1 (q, *J* = 7.1 Hz, OCH_2, 2H), 1.4 (t, *J* = 7.1 Hz, 3H), 0.91 (s, d, 6H), 0.65 (s, 3H). **^{13}C NMR** (63 MHz, $CDCl_3$) δ 180.4 (CO), 167.0 (CO), 165.0 (C), 112.6 (CH=), 59.4 (CH_2), 56.4 (CH), 55.85 (CH), 44.8 (CH), 42.7 (CH), 40.55 (CH), 40.1 (CH_2), 38.5 (CH_2), 35.7 (C), 35.2 (CH), 32.8 (CH_2), 31.0 (CH_2), 30.7 (CH_2), 30.3 (CH_2), 28.1 (CH_2), 27.1 (CH_2), 26.1 (CH_2), 24.1 (CH_2), 23.3 (C), 21.0 (CH_2), 18.2 (CH_3), 14.3 (CH_3), 14.1 (CH_3), 12.0 (CH_3). **IR** (film, cm^{-1}): 3421, 2931, 2863, 1710, 1646. **HRMS** (EI): calcd for $C_{28}H_{44}O_4Na$ $[M+Na]^+$, 467.3137; found, 467.3134. A sample of **2Z** for biological testing was purified by HPLC as indicated in general procedures (see also SI).

(3α,5β)-3-(2-Ethoxy-2-oxoethyl)-cholan-24-ol *tert*-Butyldimethylsilyl Ether (13a). Pd/C (10%, 0.088 g, 0.082 mmol, 0.1 equiv) was added to a solution of **5Z** (0.45 g, 0.827 mmol) in EtOAc (10 mL). The mixture was stirred for 12 h under H_2 (balloon pressure). The mixture was filtered through a layer of celite and rinsed with EtOAc (3x20 mL). The filtrate was concentrated to give **13a** and its C3-epimer **13b** [0.430 g, 95%, (5:1 ratio by ^{13}C-NMR), R_f = 0.7 (10% EtOAc/hexanes), colorless oil], which were separated by medium pressure column chromatography (silica VersaPak cartridges, 1% EtOAc/hexanes). Hydrogenation of a mixture of **5Z** and **5E**, prepared from **10**, under the same reaction conditions provided the same results as above. $[\alpha]^{25}_D$ +22.2 (c 1, $CHCl_3$). **^{1}H NMR** (500 MHz, $CDCl_3$) δ 4.12 (q, *J* = 7.1 Hz, 2H), 3.57 (t, *J* = 6.5 Hz, 2H), 2.20 (d, *J* = 7.1 Hz, 2H), 0.90 (s, d, 12H), 0.64 (s, 3H). **^{13}C NMR** (63 MHz, $CDCl_3$) δ 172.9 (C=O), 63.6 (O**CH_2**CH_3), 59.8 (CH_2-C24), 56.4 (CH), 56.1 (CH), 43.1 (CH), 42.5 (C), 42.1 (CH_2), 40.4 (CH), 40.1 (CH_2), 36.8 (CH_2), 35.7 (C), 35.6 (CH), 35.35 (C), 34.7 (C), 33.4 (CH_2), 31.8 (CH_2), 31.4 (CH), 29.3 (CH_2), 28.1 (CH_2), 27.4 (CH_2), 27.15 (CH_2), 26.3 (CH_2), 25.8 (C), 24.05 (CH_2), 23.7 (CH_3), 20.7 (CH_2), 18.5 (CH_3), 14.1 (CH_3), 11.8 (CH_3), -5.45 (2xCH_3). **IR** (film, cm^{-1}): 2924, 2854, 1732. **HRMS** (EI), calcd for $C_{34}H_{63}O_3Si$ $[M+H]^+$, 547.4546; found, 547.4541

(3α,5β)-3-(2-Oxoethyl-2-ethoxy)-cholan-24-ol (7a). A solution of TBAF in THF (1.06 mL, 1.06 mmol, 1M, 1.5 equiv) was added to a solution of **13a** (0.390 g, 0.713 mmol, 1 equiv) in THF (10 mL). The mixture was stirred at 23 ºC for 12 h. The reaction was quenched with saturated NaCl. The mixture was extracted with EtOAc (3x7 mL). The combined organic extracts were dried, filtered and concentrated. The residue was purified by flash chromatography (SiO_2, Ø 2×6 cm, 15% EtOAc/hexanes) to give **7a** [0.300 g, 0.699 mmol 97%, R_f = 0.31 (15% EtOAc/hexanes), white solid (mp 85-88 °C)]. $[\alpha]_D^{25}$ +28 (*c* 1.2, $CHCl_3$). **^{1}H NMR** (250 MHz, $CDCl_3$) δ 4.1 (q, *J* = 7.1 Hz, 2H, O**CH_2**CH_3), 3.55 (t, *J* = 6.3 Hz, 2H, **CH_2**OH), 2.15 (d, *J* = 7.0 Hz, 2H, CH_2CO), (m, 7H), 1.2 (t, *J* = 7.1 Hz, 3H), 0.9 (s, d, 6H), 0.59 (s, 3H). **^{13}C NMR** (63 MHz, $CDCl_3$) δ 173.13 (C=O), 63.4 (O**C**H_2CH_3)), 60.0 (O**C**H_2), 56.4 (CH), 56.01 (C, C), 43.0 (C), 42.5 (CH), 42.1 (CH_2), 40.35 (CH), 40.0 (CH_2), 36.8 (CH_2), 35.7 (C), 35.6 (CH), 35.43 (C), 34.7 (C), 33.4 (CH_2), 31.7 (CH_2), 29.2 (CH_2),

28.15 (CH_2), 27.4 (CH_2), 27.1 (CH_2), 26.3 (CH_2), 24.05 (CH_2), 23.75 (CH_3), 20.65 (CH_2), 18.5 (CH_3), 14.15 (CH_3), 11.9 (CH_3). **IR** (film, cm^{-1}): 3504, 2935, 2860, 1716. **HRMS (EI)**: calcd for $C_{28}H_{49}O_3$ $[M+H]^+$, 433.3682; found 433.3676.

(3α,5β)-3-(2-Ethoxy-2-oxoethyl)-cholan-24-oic acid (3a). Two-step oxidation as for **2E**. **3a** (110 mg, 60%, R_f = 0.32 (20% EtOAc/hexanes), white solid (mp 49–52 °C)]. $[\alpha]_D^{25}$ +31.09 (*c* 1.1, $CHCl_3$). **^{1}H NMR** (250 MHz, $CDCl_3$) δ 9.8 (brs, 1H), 4.1 (q, *J* = 7.1 Hz, 2H, O**CH_2**CH_3), 2.18 (d, *J* = 7.0 Hz, 2H), 0.89 (s, d, *J* = 3.6 Hz, 6H), 0.61 (s, 3H). **^{13}C NMR** (63 MHz, $CDCl_3$) δ 180.4 (**C**O_2Et), 173.3 (**C**O_2H), 60.1 (O**CH_2**CH_3), 56.4 (CH), 55.8 (C), 43.1 (CH), 42.6 (C), 42.2 (CH_2), 40.4 (CH), 40.1 (CH_2), 36.8 (CH), 35.7 (CH_2), 35.2 (C), 34.77 (C), 33.4 (CH_2), 30.96 (CH_2), 30.7 (CH_2), 28.1 (CH_2), 27.5 (CH_2), 27.2 (CH_2), 26.3 (CH_2), 24.10 (CH_2), 23.8 (CH_3), 20.7 (CH_2), 18.15 (CH_3), 14.2 (CH_3) 12.0 (CH_3). **IR** (film, cm^{-1}): 3435, 2929, 2856, 1731, 1713. **HRMS (EI)**: calcd for $C_{28}H_{47}O_4$ $[M+H]^+$, 447.3474; found, 47.3469. A sample of **3a** for biological testing was purified by HPLC as indicated in general procedures.

(3α,5β)-3-(2-Hydroxy-2-methylpropyl)-cholan-24-ol *tert*-Butyldimethylsilyl Ether (14a*).*** A solution of MeMgBr in Et_2O (8.1 mmol, 2.7 mL, 3M, 9 equiv) was added to a 0 °C cooled solution of **13a** (0.5 g, 0.95 mmol) in dry THF (10 mL). The cooling bath was removed. The mixture was stirred for 15 min. The mixture was concentrated in *vacuo* and the residue was extracted with EtOAc (3x10 mL). The combined organic extracts were dried, filtered and concentrated to give **14a** [0.455 g, 93%, R_f = 0.15 (10% EtOAc/hexanes), colorless oil]. $[\alpha]_{25}^{D}$ +26.1 (*c* 1.2, $CHCl_3$)]. **^{1}H NMR** (250 MHz, $CDCl_3$) δ 3.5 (brs, 2H), 1.2 (s, 6H), 0.8 (m, 12H), 0.6 (s, 3H), -0.03 (s, 6H). **^{13}C NMR** (63 MHz, $CDCl_3$) δ 71.3 (C), 63.6 (CH_2), 60.0 (C), 56.4 (CH), 56.1 (CH), 51.15 (CH_2), 43.5(CH), 42.5 (CH), 40.4 (CH), 40.10 (CH_2), 37.35 (CH_2), 35.8 CH_2), 35.7 (CH_2), 35.3 (C), 34.8 (CH_2), 34.5 (CH_2), 31.8 (CH_2), 29.8 (C), 29.6 (2xCH_3), 29.2 (CH_2), 28.1 (CH_2), 27.3 (CH_2), 26.3 (CH_2), 25.8 (3xCH_3), 24.05 (CH_2), 23.8 (CH_2), 20.7 (C), 18.5 (CH_2), 18.1 (CH_3), 11.9 (CH_3), -5.43 (2xCH_3)**. HRMS (EI**): calcd for $C_{30}H_{55}O_2Si$ $[M+H]^+$, 534.4766; found, 534.4757.

(3α,5β)-3-(2-Hydroxy-2-methylpropyl)-24-cholan-1-ol (8a). A solution of TBAF in THF (0.6 mL, 0.639 mmol, 1M, 1.5 equiv) was added to a solution of **14a** (0.227 g, 0.426 mmol, 1 equiv) in THF (0.5 mL). The mixture was stirred at 23 °C for 12 h. The reaction was quenched with saturated NaCl. The mixture was extracted with EtOAc (3x7 mL). The combined organic extracts were dried, filtered and concentrated. The residue was purified by flash chromatography (SiO_2, Ø 2.5×6 cm, 1% EtOAc/hexanes) to give **8a** [0.167 g, 97%, R_f = 0.21 (20% EtOAc/hexanes), white solid (mp 150-154 °C]. $[\alpha]_D^{25}$ +22 (*c* 1.2, $CHCl_3$). **^{1}H NMR** (250 MHz, $CDCl_3$) δ 3.6 (t, *J* = 6.5 Hz, 3H), 1.2 (s, 6H), 0.9 (s, d, *J* = 5.6 Hz, 6H), 0.6 (s, 3H). **^{13}C NMR** (63 MHz, $CDCl_3$) δ 71.5 (C), 63.4 (CH_2), 56.4 (CH), 56.0 (CH), 51.1 (CH_2), 43.5 (C), 42.5 (C), 40.4 (CH), 40.1 (CH_2, C-12), 37.3 (CH_2), 35.8 (CH), 35.7 (CH), 35.4 (C), 34.9 (CH_2), 34.6 (CH_2), 31.7 (2xCH_3), 29.9 (CH_2), 29.7, 29.2 (CH_2), 28.2 (CH_2), 27.3 (CH_2), 26.4 (CH_2), 24.1 (CH_2), 23.9 (CH_2), 20.7 (CH_3), 18.5 (CH_3), 11.9 (CH_3). **IR** (film, cm^{-1}): 3346, 2971, 2922, 2861. **HRMS (EI**) Calcd for $C_{28}H_{50}O_2Na$ $[M+Na]^+$, 441.3709; found 441.3703.

(3α,5β)-3-(2-Hydroxy-2-methylpropyl)-cholan-24-oic Acid (4a). Two-step oxidation as for **2E**. **4a** [30] [99 mg, 63%, R_f = 0.26 (25% EtOAc/hexanes), white solid (mp 151-154 °C)]. $[\alpha]_D^{25}$ = +27.6 (*c* 1, $CHCl_3$)]. **^{1}H NMR** (250 MHz, $CDCl_3$) δ 2.4-2.1 (m, 2H), 1.2 (s, 6H), 0.89 (s, d, *J* = 5.2 Hz, 6H), 0.61 (s, 3H). **^{13}C NMR** (63 MHz, $CDCl_3$) δ

179.1 (CO), 71.7 (C), 56.4 (CH), 55.8 (CH), 51.0 (CH_2), 43.5 (CH), 42.60 (CH), 40.4 (CH), 40.1 (CH), 37.3 (CH_2), 35.8 (C), 35.7 (CH), 35.2 (C), 34.9 (CH_2), 34.6 (CH_2), 30.8 (CH_2), 30.7 (2xCH_3), 29.8 (CH_2), 29.7 (CH_2), 29.7 (CH_2), 28.0 (CH_2), 27.3 (CH_2), 26.3 (C), 23.8 (CH_2), 20.7 (CH_3), 18.1 (CH_2), 11.9 (CH_2). **IR** (film, cm^{-1}): 3425, 2929, 2861, 1712. **HRMS (EI**) Calcd for $C_{28}H_{48}O_3Na$ $[M+Na]^+$, 455.3501; found 455.3496. A sample of **4a** for biological testing was purified by HPLC as indicated in general procedures.

(3β,5β)-3-(2-Ethoxy-2-oxoethyl)-cholan-24-ol (7b*).* A mixture of CuCl (0.032 mg, 0.325 mmol, 0.7 equiv), (*S*)-*tol*-BINAP (0.029 g, 0.044 mmol, 0.12 equiv), PMHS (0.354 g, 5.87 mmol, 16 equiv), and a solution of KO*t*-Bu in THF (0.20 ml, 0.275 mmol, 0.75 equiv, 1M) was sonicated for 2 h and then cooled to –20 ºC. A solution of **5Z** (0.200 g, 0.367 mmol, 1 equiv) in hexanes (4 mL) and *i*-PrOH (17 µL) were successively added. The mixture was stirred for 3.5 h. The cooling bath was removed and the mixture was allowed to reach 23 ºC. The reaction was quenched by the addition of an aqueous solution of HCl (10%, 15 ml). The mixture was extracted with EtOAc (3x25 mL). The combined organic phases were dried, filtered and concentrated. The residue was chromatographed (SiO_2, Ø 2.5x16 cm, 2% EtOAc/hexanes) to give the corresponding (3β)-saturated ester [1.13 g, 3.54 mmol, semisolid, R_f = 0.55 (2% EtOAc/hexanes)], which was subjected to deprotection and removal traces of PMHS as follows. A solution of this semisolid (0.300 g, 0.548 mmol, 1 equiv) in THF (8 mL) was treated with an aqueous solution of HF (48%, 0.15 mL). The mixture was stirred at 23 ºC for 12 h and then slowly poured onto saturated $NaHCO_3$ (50 mL). The mixture was extracted with EtOAc (3x25 mL). The combined organic phases were washed with saturated NaCl (20 mL), dried, filtered and concentrated. The residue was purified by flash chromatography (SiO_2, Ø 1.5x6 cm, 10% EtOAc/hexanes) to give **7b** [0.220 g, 0.346 mmol, 96%, white solid (mp 102-104 °C), R_f = 0.21 (10% EtOAc/hexanes)]. $[\alpha]_D^{25}$ +26.6 (c 2, $CHCl_3$)]. **^{1}H NMR** (250 MHz, $CDCl_3$) δ 4.1 (q, *J* = 6.9 Hz, 2H, O**C**H_2CH_3), 3.6 (t, *J* = 5.8 Hz, 2H, CH_2-24), 2.4 (d, *J* = 5.0 Hz, 2H, $CH_2C(O)O$), 0.9 (s, d, *J* = 5.7 Hz, 6H), 0.61 (s, 3H). **^{13}C NMR** (63 MHz, $CDCl_3$) δ 173.6 (CO), 63.4 (O**C**H_2CH_3), 59.9 (O**C**H_2), 56.4 (CH), 56.04 (CH), 42.5 (C), 40.1 (CH_2), 39.8 (CH), 37.25 (CH), 37.0 (CH_2), 35.55 (CH), 35.4 (C), 35.2 (C), 31.7 (CH_2), 30.95 (CH_2), 30.5 (CH_2), 30.3 (CH_2), 29.3 (CH_2), 28.15 (CH_2), 26.9 (CH), 26.1 (CH_2), 24.4 (CH_2), 24.00 (C), 20.7 (CH_2), 18.5 (CH_3), 14.1 (CH_3), 11.89 (CH_3). **IR** (film, cm^{-1}): 3434, 2930, 2863, 1734. **HRMS** (EI): calcd for $C_{28}H_{49}O_3$ $[M+H]^+$, 433.3682; found, 433.3676.

(3β,5β)-3-(2-ethoxy-2-oxoethyl)-cholan-24-oic Acid (3b*).* Two-step oxidation as for **2E. 3b** [0.105 g, 61%, R_f = 0.27 (12% EtOAc/hexanes), white solid]. $[\alpha]_D^{25}$ +19 (*c* 1.2, $CHCl_3$). **^{1}H NMR** (250 MHz, $CDCl_3$) δ 4.08 (q, *J* = 7.1 Hz, 2H), 1.21 (t, *J* = 7.1 Hz, 3H), 0.89 (s, 3H), 0.87 (s, 3H), 0.60 (s, 3H). **^{13}C NMR** (63 MHz, $CDCl_3$) δ 180.25 (CO), 173.7 (CO), 60.0 (CH_2), 56.4 (CH), 55.8 (C), 42.6 (C), 40.0 (CH_2), 39.8 (CH), 37.2 (CH), 37.0 (CH_2), 35.5 (CH), 35.2 (C), 31.4 (C), 30.9 (CH_2), 30.9 (CH_2), 30.6 (CH_2), 30.5 (C), 30.3 (CH_2), 28.0 (CH_2), 26.9 (CH_2), 26.1 (CH_2), 24.4 (CH_2), 24.0 (CH_2), 20.7 (CH_2), 18.08 (CH_3), 14.1 (CH_3), 14.0 (CH_3), 11.9 (CH_3). **IR** (film, cm^{-1}): 3445, 2932, 2863, 1734, 1707. **HRMS** (EI): calcd for $C_{28}H_{47}O_4$ $[M+H]^+$, 447.3474; found, 447.3469. A sample of **3b** for biological testing was purified by HPLC as indicated in general procedures.

(3β,5β)-3-(2-Hydroxy-2-methylpropyl)-(5β)-cholan-24-ol (8b). A solution of MeMgBr in Et_2O (6.240 mmol, 2.1 mL, 3M, 9 equiv) was added to a 0 ºC cooled solution of **7b** (300 mg, 0.693 mmol) in THF (10 mL). The mixture was

refluxed for 2.5 h. The reaction was quenched by addition of 5% HCl. The mixture was extracted with EtOAc (3x7 mL). The combined organic extracts were dried, filtered and concentrated. The residue was purified by flash chromatography (SiO_2, Ø 2x6 cm, 2% EtOAc/hexanes) to afford **8b [**0.282 g, 94%, R_f = 0.61 (30% EtOAc/hexanes), white solid, (mp 138-139 °C]. $[\alpha]_D^{25}$ +30.6 (*c* 1.2, $CHCl_3$). **^{1}H NMR** (250 MHz, $CDCl_3$) δ 3.5 (t, *J* = 5.7 Hz, 2H), 1.2 (s, 6H), 0.9 (s, d, 6H), 0.6 (s, 3H). **^{13}C NMR** (63 MHz, $CDCl_3$) δ 71.8 (C), 63.3 (CH_2), 56.5 (CH), 56.1 (CH), 46.05 (CH_2), 42.6 (C), 40.1 (CH_2), 39.8 (CH), 37.6 (CH), 35.6 (CH), 35.4 (CH), 34.9 (C), 32.7 (CH_2), 31.7 (CH_2), 31.4 (CH_2), 29.4 (CH_3), 29.3 (CH_3), 29.2 (CH_3), 29.2 (CH_2), 28.2 (CH_2), 27.2 (CH_2), 26.8 (CH_2), 26.3 (CH_2), 24.1 (CH_2), 20.8 (CH_2), 18.5 (CH_3), 11.9 (CH_3). **IR** (film, cm-^{1}); 3371, 2930, 2863. **HRMS** (EI): calcd for $C_{28}H_{50}O_2$ $[M+Na]^+$, 441.3709; found, 441.3703.

(3β,5β)–(2-hydroxy-2-methylpropyl)-cholan-24-oic acid (4b*).* Two-step oxidation as for **2E**. **4b** ([30] [120 mg, 55%, R_f = 0.53 (35% EtOAc/hexanes), white solid (mp 133-135 ºC)]. $[\alpha]_D^{25}$ +16.6 (*c* 1.5, $CHCl_3$). **^{1}H NMR** (250 MHz, $CDCl_3$) δ 2.4-2.2 (m, 2H), 1.25 (s, 6H), 0.91 (s, d, 6H), 0.64 (s, 3H). **^{13}C NMR** (63 MHz, $CDCl_3$) δ 179.3 (CO), 72.0 (C), 63.7 (CH_2), 56.45 (CH), 55.8 (CH), 46.0 (CH_2), 42.6 (CH_2), 40.1 (CH), 39.8 (CH), 37.6 (CH), 35.6 (CH), 35.2 (CH_2), 34.9 (C), 32.7 (CH_2), 31.4 (CH_2), 30.84 (CH_2), 30.7 (2xCH_3), 29.3 (CH_2), 29.15 (CH_2), 28.0 (CH_2), 27.2 (CH_2), 26.8 (CH_2), 26.3 (C), 24.1 (CH_2), 22.5 (CH_2), 13.9 (CH_2), 11.9 (CH_3). **IR** (film, cm-^{1}): 3375, 2931, 2863. **HRMS** (EI): calcd for $C_{28}H_{48}O_3Na$ $[M+Na]^+$, 455.3501; found, 455.3496.

3.3. Biological evaluation

Compounds. 1,25-dihydroxyvitamin D_3 (1,25D) was purchased from Cayman Europe (Tallinn, Estonia) and was dissolved in absolute ethanol to 1 mM concentration. Compound **3a** was dissolved in absolute ethanol to 20 mM, and the remaining compounds were dissolved in absolute ethanol to 50 mM concentration.

Cells. HL60 and HT-29 cells were obtained from the local cell bank at the Institute of Immunology and Experimental Therapy in Wrocław, Poland. HL60 cells were cultured in RPMI 1640 supplemented with 10% fetal calf serum (FCS), 100 units/ml penicillin and 100 µg/ml streptomycin (all Sigma, St. Louis, MO) and HT-29 adherent cultures were in DMEM supplemented with 10% FCS, 100 units/ml penicillin, and 100 µg/ml streptomycin. The cells were cultured in humidified atmosphere of 95% air and 5% CO_2 at 37° C. The cell number and viability were determined by hemocytometer counts and trypan blue exclusion. The cells were seeded at a density of 15 x 10^4 cells/ml in culture medium containing 1,25D, a studied compound or the equivalent volume of ethanol as a vehicle control.

Flow cytometry. After 96 h of incubation HL60 cells were washed in PBS/0.1% BSA, incubated for 1 h on ice with 1 µl CD14-PE (ImmunoTools, Friesoythe, Germany). Cells were washed and suspended in 350 µl of PBS/0.1%BSA prior to analysis on the Accuri C6 (Becton Dickinson, San Jose, CA). Data analysis was performed using Becton Dickinson Accuri C6 software. The assay was repeated 3-5 times. Percentages of positive cells were plotted to the graphs and EC_{50} values were calculated using GraphPad Prism 7 software (GraphPad Software, San Diego, CA).

VDR binding assay. Binding affinity to VDR was evaluated using a PolarScreenTM Vitamin D Receptor Competitor Assay Kit under manufacturer's conditions (Invitrogen, Carlsbad, CA). 1,25D and tested compounds were evaluated within the concentration range 10^{-12}-10^{-5} M. The test components were incubated for 4h at rt in order to reach equilibrium. The polarized fluorescence of every plate was measured three times using Envision multiplate reader (PerkinElmer, Waltham, MA) and mean fluorescence polarization was calculated from these measurements. The whole assay was repeated three times. IC_{50} values were calculated in GraphPad Prism 7 using the average of values obtained.

Western blotting. In order to obtain cytosolic and nuclear extracts $6x10^6$ HL60 cells/sample were washed and lysed using NE-PER Nuclear and Cytoplasmic Extraction Regents (Thermo Fisher Scientific Inc., Worcester, MA) according to the user's manual. Lysates were denatured by adding 5x sample buffer (1/4 volume of the lysate) and boiled for 5 min. 20 µl of each lysate were separated in SDS-PAGE and electroblotted to PVDF membrane. The membranes were then dried and incubated sequentially with primary anti-VDR and anti-HDAC2 (both from Santa Cruz Biotechnology Inc.; Santa Cruz, CA, USA) and a horseradish peroxidase-conjugated anti-mouse secondary antibody (Jackson ImmunoResearch; Cambridgeshire, UK). The protein bands were visualized with chemiluminescence (Santa Cruz). Then the membranes were stripped, dried again and probed with subsequent antibodies.

cDNA synthesis and real time PCR. Total RNA was isolated using EXTRAzol reagent (BLIRT S.A., Gdańsk, Poland) according to the manufacturer's recommendations. RNA quantity was determined using Nanodrop (Thermo Fisher Scientific Inc. Worcester, MA) and the quality of RNA was verified by gel electrophoresis. RNA was transcribed into cDNA using High Capacity cDNA Reverse Transcription kit (Applied Biosystems, Foster City, CA). Real Time PCR was performed using SensiFAST™ SYBR Hi-ROX Kit (Bioline, London, UK) in CFX Connect Real-Time PCR Detection System (Bio-Rad Laboratories, Inc., Hercules, CA). The sequence of *CYP24A1* primers were (fp): 5'-CTCATGCTAAATACCCAGGTG-3', (rp): 5'-TCGCTGGCAAAACGCGATGGG-3', *CD14* (fp): 5'-GTTCGGAAGACTTATCGACCATGGAGC-3', (rp): 5'-CAGACGCAGCGGAAATCTTCATC-3', *TRPV6* (fp): 5'- TGT ACT TCG CCC GAG GAT TC-3', (rp): 5'- ATA GAA GGC TGA AGC AAA GCC-3', while sequences of *GAPDH* were as follow: (fp): 5'-CAT GAG AAG TAT GAC AAC AGC CT-3', (rp): 5'-AGT CCT TCC ACG ATA CCA AAG T-3'. Fold changes of mRNA levels in *CYP24A1*, *CD14* or *TRPV6* genes relative to the *GAPDH* gene were calculated by relative quantification analysis [50].

Calcemic activity. The calcemic activity of the compound 4a was evaluated in 8-week old female NMRI mice (Charles River Laboratories, Belgium) by daily intraperitoneal administration of 1,25D, 4a or the solvent (arachis oil) for 7 consecutive days (n=5 per experimental group). 24 h after the last injection, mice were sacrificed and serum was collected. Serum calcium concentration, measured with a Beckman Coulter AU640 chemistry analyzer (Arsenazo III assay, Analis, Belgium), was used as endpoint for the assessment of calcemic activity. Mice were housed in an animal facility with 12 h dark/light cycles and constant temperature. Food (containing 1% calcium, 0.7% phosphate, and 1100 IU/kg vitamin D, Snniff, Soest, Germany) and water were supplied ad libitum. The protocol for the evaluation of calcemic activity was approved by the ethical committee for animal research at the KU Leuven.

Analysis of the results. Microsoft Excel and GraphPad Prism 7 software were used to analyze the results. For statistical analysis of differences between untreated and treated samples Student's t-test for independent samples was used. In order to test if samples treated with the compounds were significantly different from 1,25D-treated samples, one-way ANOVA followed by Dunnett post hoc analysis were used.

3.4. Crystallization and structure determination

Expression of zebrafish VDR LBD (residues 156–453) and the following purification were done by the procedure reported previously [40]. The protein was concentrated using Amicon ultra-30 (Millipore) to 3-7 mg/ml and incubated with a two-fold excess of ligand and a three-fold excess of the coactivator SRC-1 NR2 (686-RHKILHRLLQEGSPS-700) peptide (IGBMC peptide synthesis common facility). Crystals were obtained in 50 mM Bis-Tris pH 6.5, 1.6 M lithium sulfate and 50 mM magnesium sulfate. Protein crystals were mounted in a fiber loop and flash-cooled under a nitrogen flux after cryo-protection with 20% glycerol. Data collection from a single frozen crystal was performed at 100 K on the PX2A beamline at SOLEIL (France). The raw data were processed with XDS [51] and scaled with AIMLESS [52] programs. The crystals belong to the space group $P6_522$, with one LBD complex per asymmetric unit. The structure was solved and refined using Phenix [53] and iterative model building using COOT [54]. Crystallographic refinement statistics are presented in Supplementary data.

Associated content

Supporting Information (SI). Molecular docking tables, ^{1}H NMR and ^{13}C NMR spectra, X-ray crystallographic data of all compounds and HPLC purity data for **2E** and **2Z**. These data can be found online at https://doi.org/

Declaration of Competing Interest

The authors declare no competing financial interest.

Acknowledgement

We thank Xunta de Galicia (GRC/ED431B/ 2018/13) for financial support. We also thank institutional funds from Instruct-ERIC for support and use of resources of the French Infrastructure for Integrated Structural Biology (ANR-10-LABX-0030-INRT and ANR-10-IDEX-0002-02). We thank Prof. M.A. Maestro for the X-ray studies, Dishman-Netherlands B.V. for the gift of vitamin D_2, P. Eberling for peptide synthesis, A. McEwen for help in X-ray data collection and the staff of PX2 beamline of SOLEIL synchrotron for assistance during X-ray data collection. S.G. thanks the European Union for an Erasmus Mundus Euphrates scholarship (Project 2013-250/001-001-EMA2). K.B. and E.M. were supported by the Leading National Research Center Poland (KNOW).

Abbreviations used

1,25D, 1α,25-dihydroxyvitamin D_3; 1,25D, 1α,25-dihydroxyvitamin D_3; VDR, vitamin D receptor; LBD, ligand binding domain. BSA, bovine serum albumin; CD-14, cluster of differentiation 14; CYP24A1, cytochrome P450 family 24 subfamily A member 1; DMEM, Dulbecco's modified Eagle medium; EMR, effective molar ratio; FCS, fetal calf serum; GAPDH, glyceraldehyde 3-phosphate dehydrogenase; HDAC2, histone deacetylase 2, LBD, ligand binding domain; PBS, phosphate buffered saline; PE, phycoerythrin; RBA, relative binding affinity; PVDF,

polyvinylidene difluoride; RPMI, Roswell Park Memorial Institute medium; TRPV6, transient receptor potential cation channel subfamily V member 6; SDS-PAGE, sodium dodecyl sulphate–polyacrylamide gel electrophoresis; VDR, vitamin D receptor; *tol*-BINAP = 2,2'-Bis(di-*p*-tolylphosphino)-1,1'- binaphthalene; KO*t*-Bu, potassium *tert*-butoxide; TBS, *tert*-butyl dimethyl silyl; TBME, *tert*-butyl methyl ether; EtOAc, DMF: dimethyl formamide; EtOAc, ethyl acetate; IR, infrared spectrum; MeMgCl, methylmagnesium chloride; NMR, nuclear magnetic spectrum; PDC, pyridinium dichromate; Oxone®, potassium peroxymonosulfate; PMHS, polymethylhydrosiloxane; *Rt*, retention factor; *p*-Ts, paratoluenesulfonyl; TBAF, *n*-tetrabutylammonium fluoride. THF, tetrahydrofuran. MeMgCl, methylmagnesium chloride. MPLC, Medium pressure liquid chromatography.

References

[1] R.M. Evans, Steroid and thyroid hormone receptor superfamily, Science 240 (1988) 889–895.

[2] G. Jones, S.A. Strugnell, H.F. DeLuca, Current understanding of the molecular actions of vitamin D, Physiol. Rev. 78 (1998) 1193–1231.

[3] M.R. Haussler, G.K. Whitfield, I. Kaneko, C.A. Haussler, D. Hsieh, J-C. Hsieh, P.W. Jurutka. Molecular mechanisms of vitamin D action. Calcif, Tissue Int. 92 (2013) 77–98.

[4] Vitamin D (D. Feldman, J.W. Pike, J.S. Adams). Two-Volume Set, Elsevier, Academic Press, New York, 2011.

[5] S. Li, J. De La Cruz, S. Hutchens, S. Mukhopadhyay, Z.K. Criss, R. Aita, O. Pellon-Cardenas, J. Hur, P. Soteropoulos, S. Husain, P. Dhawan, L. Verlinden, G. Carmeliet, J.C. Fleet, N.F. Shroyer, M.P. Verzi, S. Christakos, Analysis of 1,25-Dihydroxyvitamin D_3 Genomic Action Reveals Calcium-Regulating and Calcium-Independent Effects in Mouse Intestine and Human Enteroids, Mol Cell Biol. 41 (2020) e00372-20.

[6] S.V. Ramagopalan, A. Heger, A.J. Berlanga, N.J. Maugeri, M.R. Lincoln, A. Burrell, L. Handunnetthi, A.E. Handel, G. Disanto, S-M. Orton, C.T. Watson, J.M. Morahan, G. Giovannoni, C.P. Ponting, G.C. Ebers, J.C. Knight. A ChIP-seq defined genome-wide map of vitamin D receptor binding: associations with disease and evolution. Genome Research 20 (2010) 1352-1360.

[7] F. Pereira, M.J. Larriba, A. Muñoz. Vitamin D and colon cancer. Endocrine-Related Cancer 19 (2012) R51–R71.

[8] M.A. Maestro, F. Molnar, C. Carlberg, Vitamin D and its synthetic analogs, J. Med. Chem. 62 (2019) 6854-6875.

[9] J. Chen, Z. Tang, A.T. Slominski, W. Li, M.A. Żmijewski, Y. Liu, J. Chen, Vitamin D and its analogs as anticancer and anti-inflammatory agents, Eur J Med Chem. 207 (2020) 112738.

[10] A. Lori, L.A. Plum, H.F. DeLuca, Vitamin D, disease and therapeutic opportunities, Nat. Drug Discov. 9 (2010) 941-955.

[11] C. Leysserns, L. Verlinden, M. Verstuyf, The future of vitamin D analogs, Front. Physiol. 5 (2014) 1-18.

[12] M.J. Calverly, Synthesis of MC 903, a biologically active vitamin D metabolite, Tetrahedron 43 (1987) 4609-4619.

[13] R.K Jain, D.L. Trump, M.J. Egorin, M. Fernandez, C.S. Johnson, R.K. Ramanathan, A phase I study of the vitamin D_3 analogue ILX23-7553 administered orally to patients with advanced solid tumors, Invest. New Drugs 29 (2011) 1420-1425.

[14] R. Sigüeiro, M.A. Maestro, A. Mouriño, Synthesis of side-chain locked analogs of 1α,25-dihydroxyvitamin D_3 bearing a C17 methyl group, Org. Lett. 20 (2018) 2641-2644.

[15] P. Gogoi, S. Seoane, R. Sigüeiro, T. Guiberteau, M.A. Maestro, R. Pérez-Fernández, N. Rochel, A. Mouriño, Aromatic-Based Design of highly active and noncalcemic vitamin D receptor agonists, J. Med. Chem. 61 (2018) 4928-4937.

[16] A. Glebocka, G. Chiellini, A-ring analogs of 1,25-dihydroxyvitamin D_3, Arch. Biochem. Biophys. 523 (2012) 48-57.

[17] L. Verlinden, A. Verstuyf, M. Van Camp, S. Marcelis, K. Sabbe, X.-Y. Zhao, P. De Clercq, M. Vandewalle, R. Bouillon, Two novel 14-epi-analogues of 1,25-dihydroxyvitamin D_3 inhibit the growth of human breast cancer cells in vitro and in vivo, Cancer Res. 60 (2000) 2673-2679.

[18] K. Ono, A. Yoshida, N. Saito, T. Fujishima, S. Honzawa, Y. Suhara, S. Kishimoto, T. Sugiura, K.W. Aku, H.T. Takayama, A. Kittaka, Efficient synthesis of 2-modified 1 alpha,25-dihydroxy-19-norvitamin D3 with Julia olefination: high potency in induction of differentiation on HL-60 cells, J. Org. Chem. 68 (2003) 7407-7415.

[19] S. Yamada, M. Makishima, Structure–activity relationship of nonsecosteroidal vitamin D receptor modulators, Trends Pharmacol. Sci. 35 (2014) 324-337.

[20] A.Y. Belorusova, N. Rochel, Structural Studies of Vitamin D Nuclear Receptor Ligand-Binding Properties, Vitam Horm. 100 (2016) 83-116.

[21] MF. Boehml, P. Fitzgerald, A. Zou, M.G. Elgort, E.D. Bischoff, L. Mere, D.E. Mais, R.P. Bissonnette, R.A. Heyman, A.M. Nadzanl, M. Reichman E.A. Allegretto, Novel nonsecosteroidal vitamin D mimics exert VDR-modulating activities with less calcium mobilization than 1,25-dihydroxyvitamin D_3, Chem. Biol. 6 (1999) 265-275.

[22] F. Ciesielski, Y. Sato, Y. Chebaro, D. Moras, A. Dejaegere, N. Rochel, Structural basis for the accommodation of bis- and tris-aromatic derivatives in the vitamin D nuclear receptor, J. Med. Chem. 55 (2012) 8440-8449.

[23] S. Fujii, R. Sekine, A. Kano, H. Masuno, S. Songkram, E. Kawachi, T. Hirano, A. Tanatani, H. Kagechika, Structural development of p-carborane-based potent non-secosteroidal vitamin D analogs, Bioorg. Med. Chem. 22 (2014) 5891-5901.

[24] A.T. Slominski, T.K. Kim, W. Li, A. Postlethwaite, E.W. Tieu, E.K.Y. Tang, R.C. Tuckey, Detection of novel CYP11A1-derived secosteroids in the human epidermis and serum and pig adrenal gland, Sci Rep.5 (20156) 14875.

[25] M.I. Ahmad, R.R. Raghuvanshi, S. Singh, A.A. Johan, R. Prakash, K.S. Nainawat, D. Singh, S. Tripathi, A. Sharma, A. Gupta, Design and synthesis of 3-arylbenzopyran based non-steroidal vitamin-D_3 mimics as osteogenic agents, Med. Chem. Commun. 7 (2016) 2381-2394.

[26] A M. Vertino, C.M. Bula, J-R. Chen, M. Almeida, L. Han, T. Bellido, S. Kousteni, A.W. Norman, S.C. Manolagas, Nongenotropic, anti-Apoptotic signaling of 1α,25$(OH)_2$-vitamin D_3 and analogs through the ligand binding domain of the vitamin D receptor in osteoblasts and osteocytes, Chem. Biol. 280 (2005) 14130-14137.

[27] F. Chen, Q. Su, M. Torrent, N. Wei, N. Peekhaus, D. McMasters, J. Fisher, H. Glantschnig, P. Hodor, O. Flores, A. Reszka, Identification and characterization of a novel non-secosteroidal vitamin D receptor ligand, Drug Dev. Res. 68 (2007) 51-60.

[28] M. Makishima, T.T. Lu, W. Xie, G.K. Whitfield, H. Domoto, R.M. Evans, M.R. Haussler, D.J. Mangelsdorf, Vitamin D receptor as an intestinal bile acid sensor. Science. 296 (2002) 1313-1316.

[29] N. Rochel, J.M. Wurtz, A. Mitschler, B. Klaholz, D. Moras, The crystal structure of the nuclear receptor for vitamin D bound to its natural ligand, Mol. Cell 5 (2000) 173-179.

[30] P. Antony, R. Sigüeiro, T. Huet, Y. Sato, N. Ramalanjaona, L.C. Rodrigues, A. Mouriño, D. Moras, N. Rochel, Structure-function relationships and crystal structures of the vitamin D receptor bound 2-methyl-20S,23S- and 23R epoxymethano-1,25-dihydroxyvitamin D_3, J. Med. Chem. 53 (2010) 1159-1171.

[31] R. Riveiros, A. Rumbo, L.A. Sarandeses, A. Mouriño, Synthesis and conformational analysis of new 17,21-cyclo-22-unsaturated analogues of calcitriol, J. Org. Chem. 72 (2007) 5477-5485.

[32] M. Makishima, S. Yamada, The bile acid derivatives lithocholic acid acetate and lithocholic acid propionate are functionally selective vitamin D receptor ligands. In Vitamin D, 3rd ed.; Feldman, D. et al., eds.; Academic Press, 2011, pp. 1509-1524.

[33] J. A. Nehring, C. Zierold, H.F. DeLuca, Lithocholic acid can carry out in vivo functions of vitamin D, PNAS 104 (2007) 10006-10009.

[34] A. Gafar, M. Bashandy, S. Bakry, M.A. Khalifa, W.A. Walid Abu Shair, Lithocholic acid induces extrinsic apoptosis in prostate cancer cell lines, Cancer Biol. 6 (2016) 63-68.

[35] T.H. Luu, J.M. Bard, D. Carbonnelle, C. Chaillou, J.M. Huvelin, C. Bobin-Dubigeon, H. Nazih, Lithocholic bile acid inhibits lipogenesis and induces apoptosis in breast cancer cells, Cell Oncol (Dordr). 41 (2018) 13-24.

[36] T.W.H. Pols, T. Puchner, H.I. Korkmaz, M. Vos, M.R. Soeters, C.J.M. de Vries, Lithocholic acid controls adaptive immune responses by inhibition of Th1 activation through the Vitamin D receptor, Plos One 12 (2017) 1-16.

[37] M. Ishizawa, M. Matsunawa, R. Adachi, S. Uno, K. Ikeda, H. Masuno, M. Shimizu, K-I. Iwasaki, S. Yamada, M. Makishima, Lithocholic acid derivatives act as selective vitamin D receptor modulators without inducing hypercalcemia, J. Lipid Res. 49 (2008) 763-772.

[38] H. Sasaki, H. Masuno, H. Kawasaki, A.Yoshihara, N. Numoto, N. Ito, H. Ishada, K. Yamamoto, N. Hirata, Y. Kanda, E. Kawachi, H. Kagechika, A. Tanatani. Lithocholic acid derivatives as potent receptor agonists, J. Med. Chem**.** 64 (2021) 516-526.

[39] H. Masuno, T. Ikura, D. Morizono, I. Orita, S. Yamada, M. Shimizu, N. Ito, Crystal structures of complexes of vitamin D receptor ligand-binding domain with lithocholic acid derivatives, J. Lipid Res. 54 (2013) 2206-2213.

[40] A.Y. Belorusova, J. Eberhardt, N. Potier, R.H. Stone, A. Dejaegere, N. Rochel, Structural insights into the molecular mechanism of vitamin D receptor activation by lithocholic acid involving a new mode of ligand recognition, J. Med. Chem. 57 (2014) 4710-4719.

[41] A. Valkonen, E. Sievänen, S. Ikonen, N.V. Lukashev, P.A Donez, A.D. Averin, M. Lahtinen, E. Kolehmainen, Macrocyclic bile acids: from molecular recognition to degradable biomaterial, J. Mol. Struct. 846 (2007) 65-73.

[42] T. Ishikura, T. Ito, Preparation of anticancer steroid compounds having high and selective transferability to cancer tissues. Jpn. Kokai Tokkyo, Koho (1996), JP 08268917 A 19961015.

[43] When this work was in progress a patent on this compound appeared: A. Tanatani, H. Sasaki, H. Kawasaki, H. Kagechika, H. Masuno, Preparation of 3-(hydroxyalkyl)-3-dexoyIithocholic acid derivatives having vitamin activity. International Patent WO2017131144 A1 201170803, Jan 27, 2017.

[44] D.H. Appella, Y. Moritani, R. Shintani, E.M. Ferreira, S.L. Buchwald, Asymmetric conjugate reduction of α,β-unsaturated esters using a chiral phosphine-copper catalyst, J. Am. Chem. Soc. 121 (1999) 9473-9474.

[45] G. Hughes, M. Kimura, S.L. Buchwald, Catalytic enantioselective conjugate reduction of lactones and lactams. J. Am. Chem. Soc. 125 (2003) 11253-11258.

[46] M. Triantafilou, K. Triantafilou. Lipopolysaccharide recognition: CD14, TLRs and the LPS-activation cluster, Trends Immunol. 23 (2002) 301-304.

[47] H. Baurska, A. Kłopot, M. Kiełbiński, A. Chrobak, E. Wijas, A. Kutner, E. Marcinkowska, Structure-function analysis of vitamin D2 analogs as potential inducers of leukemia differentiation and inhibitors of prostate cancer proliferation, J. Steroid Biochem. Mol. Biol. 126 (2011) 46-54.

[48] T. Nijenhuis, J. Hoenderop, B. Nilius, R. Bindels, (Patho)physiological implications of the novel epithelial Ca2+ channels TRPV5 and TRPV6, Pflugers Arch. 446 (2003) 401-409.

[49] M. Meyer, M. Watanuki, S. Kim, N. Shevde, J. Pike, The human transient receptor potential vanilloid type 6 distal promoter contains multiple vitamin D receptor binding sites that mediate activation by 1,25-dihydroxyvitamin D3 in intestinal cells, Mol. Endocrinol. 20 (2006) 1447-1461.

[50] K. Livak, T. Schmittgen, Analysis of relative gene expression data using real-time quantitative PCR and the 2(-Delta Delta C(T)) method, Methods, 25 (2001) 402-408.

[51] W. Kabsch, Software XDS for image rotation, recognition and crystal symmetry assignment, Acta Crystallogr D Biol Crystallogr. 66 (2010) 125-132.

[52] P. Evans, Scaling and assessment of data quality. Acta Crystallogr. D. Biol. Crystallogr. 62 (2006) 72-82.

[53] P.V. Afonine, R.W. Grosse-Kunstleve, P.D. Adams, CCP4 Newsl 42 (2005) contribution 8.

[54] P.K. Emsley, K. Cowtan, Coot: model-building tools for molecular graphics, Acta Crystallogr D60 (2004) 2126–32.